polypeptides with a high affinity to silica from the diatom *Navicula pelliculosa*.[121]

The R5 peptide, a synthetic polypeptide derived from silaffin-1A$_1$,[122,123] as well as synthetic propylamines derived from silaffins[124] have been used to synthesize bioinspired organic-inorganic nanocomposites. The results indicate that even the nonphosphorylated protein is able to promote silica deposition. The R5 peptide has also been used in the form of a chimeric protein with the self-assembling domain of the MaSp1 protein of spider dragline silk for the synthesis of nanocomposites.[125]

4.2.2 Polyamines

Another group of molecules involved in biosilicification in diatoms are linear long-chain polyamines (molecular mass < 3.5 kDa) which have been identified in several diatom species.[16] These long-chain polyamines consist of up to 20 repeats of N-methylaminopropyl or aminopropyl units (Scheme 2). They seem to be species-specific and represent the main organic constituent of the cell walls of diatoms and occur either alone or together silaffins.

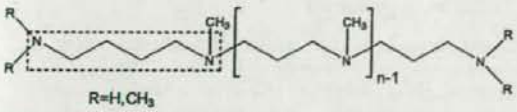

Scheme 2 Chemical structure of polyamines.

Studies of Sumper and Lehmann[126] revealed a great structural variety of the long-chain polyamines involved in silica precipitation in diatoms. The mechanism of silica precipitation from orthosilicic acid solutions induced by polyamines is not completely understood. Mizutani *et al.*[23] proposed that polycondensation of silicic acid by synthetic polyamines (polyallylamine and poly-L-lysine) follows a catalytic mechanism. It is hypothesized that, at pH 8.5, the polyamine acts as an acid-base catalyst facilitating the condensation reaction.

A catalytic mechanism for the polyamine-mediated hydrolysis and condensation of organosilicates, which resembles the mechanism proposed for silicatein, has also been proposed by Delak and Sahai.[127] It is assumed that the conjugate base of the amine performs a nucleophilic attack on the silicon to form a pentacoordinate reactive intermediate. The second amine group then forms a hydrogen bond to a water molecule, facilitating hydrolysis of the intermediate. The condensation step is thought to occur by an acid-catalyzed S_N2 mechanism.

Phosphate ions can induce the self-assembly of polyamines.[128-130] Polyamines exhibit amphiphilic properties. The aggregation and phase separation of polyamines in solution could be explained by the electrostatic interactions between the positively charged polyamine molecules and the negatively charged phosphate ions.[129] In addition, formation of hydrogen bonds may occur. The aggregates (microemulsions) formed in aqueous solution have positively charged surfaces. Multivalent anions can promote the formation of higher-order assemblies of the polyamine droplets. Silicic acid present in the aqueous phase could adsorb to the surface of the droplets, resulting in coacervate formation and finally silica formation. Based on these properties, Sumper[131] proposed a model for silica nanosphere formation and nanopatterning in diatoms, which is based on multiple phase separation processes. The characteristic "honeycomb"-like larger structures which are initially formed during silica formation are step-wise transformed into smaller structures, mediated by subsequent phase separation processes. An alternative "upscaling" model based on the results of *in situ* time-resolved ultrasmall angle X-ray scattering analyses has been proposed by Vrieling *et al.*[132]

4.3 Higher plant proteins

Early analysis of plant biosilica in *Phalaris canariensis* (canary grass) and *Equisetum telmateia* revealed low levels of entrapped proteins but also monosaccharides.[133] Model studies of silica precipitation using silicon catecholate complex as the source of soluble silicic acid showed that protein containing biosilica extracts from *Equisetum telmateia* influence the kinetics of the early stages of the silica oligomerisation.[134] These proteins present in extracts from higher plants have not yet been well characterized.

5 Biosilica dissolution

5.1 Sponges: Silicase

Sponges contain also an enzyme which is able to etch or dissolve silica. Dissolution of intact spicules is comparaby slow but seems to be faster at the ends of spicules which were mechanically broken.[135] Sponges may also be able to digest diatom frustules as has been observed in vacuoles of mobile cells of the freshwater sponge *E. fluviatilis*.[136]

The cDNA encoding the silica-catabolic enzyme, termed silicase, has been isolated from the marine sponge *S. domuncula*. This enzyme is able to dissolve amorphous silica releasing free silicic acid.[51] The expression of the silicase gene is strongly upregulated in the presence of exogenous silicate (60 µM), like the expression of silicatein.[8] The deduced polypeptide (43 kDa) is closely related to the carbonic anhydrases; the characteristic eukaryotic-type carbonic anhydrase signature is also present in the sponge enzyme (Fig. 8).[51] Carbonic anhydrases are a family of zinc metal enzymes.[137] The three conserved histidine residues which bind the zinc ion are present in the deduced amino acid sequence of silicase at aa$_{181}$, aa$_{183}$ and aa$_{206}$ (Fig. 8; and structure obtained by computer modeling, Fig. 5B).

The proposed mechanism of silicase reaction follows the mechanism of other zinc-dependent enzymes involved in ester hydrolysis (Fig. 9).[51] The reaction is initiated by a hydroxide ion which is bound to the zinc ion (a Lewis acid) and formed by splitting of the water molecule (a Lewis base). The hydroxide ion performs a nucleophilic attack at one of the silicon atoms of the polymeric silicate. Thereby the zinc-complex binds to the silicon and the oxygen bond in the polymeric silicate is cleaved. The transiently formed zinc-bound silicate is then hydrolyzed by water, resulting in the

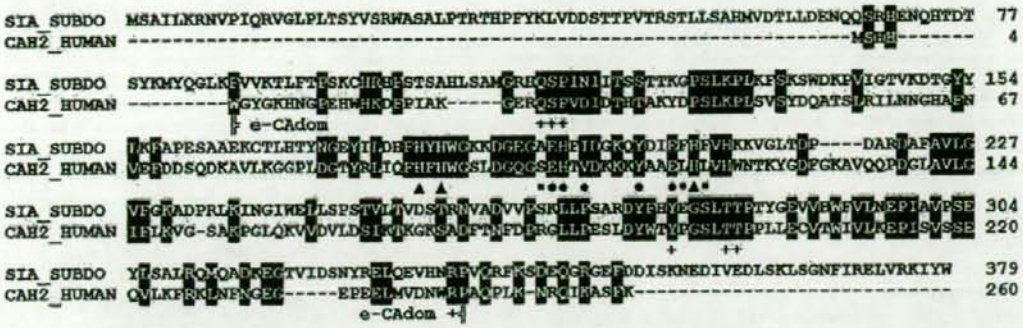

Fig. 8 Sponge silicase. Alignment of the silicase from the sponge *S. domuncula* (SIA_SUBDO) with the human carbonic anhydrase II (CAH2_HUMAN). The carbonic anhydrase domain is framed (╟ e-CAdom ╢). Similar amino acid residues in both sequences are shown in white on black. The three zinc-binding histidine residues (▲; red) and the characteristic amino acids forming the eukaryotic-type carbonic anhydrase signature (•, found in both sequences; ■, present only in the carbonic anhydrases but not in the silicase) are indicated; +, residues forming the active-site hydrogen network.

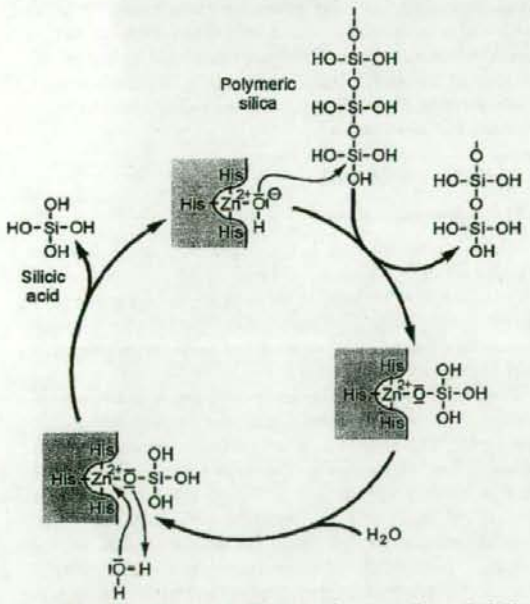

Fig. 9 Proposed mechanism of silicase reaction. According to Ref. 51 with modifications.

release of silicic acid and regeneration of the zinc-bound hydroxide.

5.2 Diatoms

A silicase, like the sponge enzyme, has not been identified in diatoms. A ferredoxin-NADP reductase (a zinc-binding protein) has been detected among the proteins from *N. pelliculosa*, that show high affinity for solid silica.[138] Although the deduced amino acid sequence of ferredoxin-NADP reductase from *Thalassiosira pseudonana* was found to be homologous with carbonic anhydrase and sponge silicase, no evidence has been found for an involvement of this enzyme in silica dissolution.[138] However, it has been demonstrated that diatoms when encapsulated into artificial silica sol-gel matrices are able to dissolve the surrounding silica.[139]

6 Silicic acid transport

Aqueous organisms live in an environment which is undersaturated with respect to silica. The average concentrations of dissolved silicon in seawater, which is mostly present as undissociated orthosilicic acid, $Si(OH)_4$, is about 70 μM.[5] In surface waters this concentration is even lower (< 3 μM) due to the biological consumption of $Si(OH)_4$.[5,140] On the other hand, the intracellular concentrations of silicon, e.g. in diatoms, can reach >100 mM,[141] thus exceeding the extracellular silicon concentration by >1000-fold. This can be seen as an indication that these organisms have developed efficient mechanisms for the active uptake of silicic acid from the surrounding water to form their silica skeleton. The uptake of silicon into sponge cells[84] and diatoms is linked to the transport of sodium.[142,143]

6.1 Sponge silicic acid transporter

The uptake of silicic acid into sponge cells is an energy consuming process.[144] The technique of differential display of mRNA from primmorphs (*S. domuncula*) that had been incubated in the absence and presence of exogenous silicate (60 μM) was used to isolate the cDNA encoding the putative silicic acid transporter.[84] The sponge transporter displays high sequence similarity to the Na^+/HCO_3^- (NBC) cotransporter; both transporters are inhibited by the stilbene compound DIDS (Fig. 10A).[84] The expression of the sponge transporter ($Na^+/HCO_3^-[Si(OH)_4]$ or NBCSA cotransporter) is strongly up-regulatated in response to increased concentrations of silicic acid (60 μM) in those sponge cells that are located adjacent to the spicules.[84] The $Na^+/HCO_3^-[Si(OH)_4]$ cotransporter in sponges is not identical with the silicon transporter in diatoms[143] (reviewed in Ref. 116). The activities of both transporters seem, however, to depend on the presence of sodium ions (sodium/silicic acid symport).

The Na^+-driven transport of silicic acid depends on the supply of ATP required for Na^+ K^+ ATPase activity to

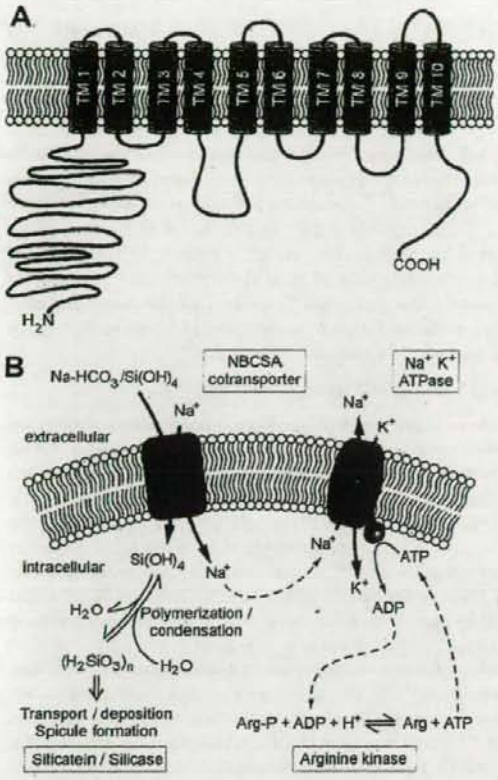

Fig. 10 (A) Predicted structure of the sponge silicic acid transporter (*S. domuncula*). The cylinders indicate ten transmembrane segments TM1-TM10. The larger intracellular loop is located between TM4 and TM5. (B) Schematic presentation of silicic acid transport in sponge cells mediated by the Na^+-driven $Na^+/HCO_3^-[Si(OH)_4]$ cotransporter (NBCSA cotransporter). The orthosilicic acid in the cytoplasm undergoes polymerization/condensation during spicule formation. The sodium gradient is maintained by Na^+ K^+ ATPase. ATP is supplied by arginine kinase reaction, which functions as phosphagen kinase in sponge cells.

maintain the sodium gradient. ATP is most likely supplied by arginine phosphate mediated by the sponge arginine kinase activity.[144] Fig. 10B shows a schematic presentation of the concerted action of the $Na^+/HCO_3^-[Si(OH)_4]$ cotransporter and arginine kinase. The expression and activity of this kinase in sponge primmorphs are increased in the presence of silicic acid.[144]

Silicon transport and spicule formation in sponges are inhibited by germanium at a Ge/Si molar ratio of 1.0.[145-147] At lower Ge/Si ratios, the growth of the spicules in length but not in width is inhibited, resulting in shorter spicules with normal morphology.[148]

6.2 Diatom silicic acid transporter

The silicon transporter from the marine pennate diatom, *C. fusiformis*, consisting of a family of five silicic acid transporters (SIT1–5) has been identified and characterized by Hildebrand *et al.*[149,150] The amino acid sequences deduced from the SIT genes contain 12 putative transmembrane segments, a signature amino acid sequence for sodium symporters and a long hydrophilic carboxy-terminus (Fig. 11A).[149,151]

The less conserved carboxy-terminal segment of the SITs has a predictable coiled-coil structure. It is assumed that this segment of the molecule interacts with other proteins or other SITs and may be involved in the control of the activity of the protein.[150] The transmembrane domain contains nine conserved cysteine residues which may explain the sensitivity of silicon transport to sulfhydryl blocking agents.[142] The silicon transporter in diatoms acts as a co-transporter with sodium ions with a 1:1 ratio of $Si(OH)_4$:Na^+.[143] The expression patterns of the five SIT genes change during the cell cycle and are correlated with the silica deposition.[150,152] The diatom silicon transporter shares no similarity with the sponge silicon transporter which is related to the Na^+/HCO_3^- (NBC) cotransporter, and the rice silicon transporter which is an aquaporin homolog (see Section 6.3). SIT homologs have also not been found in sponges.

The activity of the diatom silicon transporter was determined in *Xenopus laevis* oocytes which had been microinjected with SIT1 RNA.[149] The uptake of ^{68}Ge, which was used as an isotopic tracer for silicon, into the oocytes was abolished by silicic acid, as revealed in competition experiments, and was sodium dependent.[149] It was inhibited by sulfhydryl blockers like N-ethyl malemide.

Two models have been proposed for SIT-mediated silicon transport. The first model is based on the identification of a conserved sequence motif, CMLD, in the deduced amino acid sequences of the silicic acid transport proteins from four diatom species.[153] Grachev *et al.*[154] proposed that the functional groups in the side chains of the C, M and D residues of the conserved CMLD motif act as a potential binding site for a Zn^{2+} ion. Zinc has been shown to affect the uptake of silicic acid by diatoms.[155] It is hypothesized that the bound Zn^{2+} acts as a Lewis acid and is involved in binding and transport of silicic acid by facilitating the nucleophilic attack of a functional group of the transporter (or of another silicic acid molecule) at the silicon atom. This mechanism is similar to that proposed for the sponge silicase.[51]

However, it should be noted that the conserved cysteine residue is not found in all SIT species.[156] The authors assume that SIT species which carry a substitution of cysteine by alanine are inactive and not involved in silicic acid transport.[154]

Another model for silicon transport proposed by the group of Hildebrand is based on sequence comparison of SIT genes from eight diatom species (centrics and pennates); a conserved motif, GXQ (X = Q, G, R, or M) has been identified in four distinct regions of the deduced proteins.[156] Two of these motifs are located in predicted transmembrane sequences TM7 and TM8 (Fig. 11B). It is assumed that the (two) carbonyl groups in the side chains of the glutamine residues of the two conserved GXQ motifs in TM7 and TM8 (either alone or together with the amine groups) form hydrogen bonds to the hydroxyl groups of the silicic acid

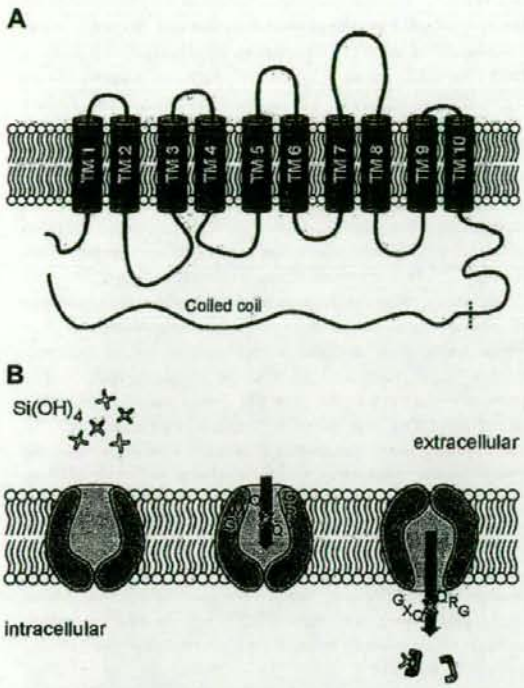

Fig. 11 (A) Predicted structure of the diatom silicic acid transporter (*C. fusiformis*) comprising ten transmembrane domains (TM1-TM10). The position of the coiled coil region is indicated. According to Ref. 225 with modifications. (B) Model of SIT-mediated silicon transport. The sequential conformational changes of the silicon transporter occurring during silicic acid transport are shown. (i) Binding of extracellular silicic acid through hydrogen bonding by two conserved glutamine residues located in transmembrane segments TM7 and TM8. (ii) Induction of a conformational change of the transporter allowing binding of silicic acid to two additional conserved glutamine residues located in the loop between TM2 and TM3. (iii) Release of silicic acid into the cell and binding to an unknown cellular component. According to Ref. 156 with modifications.

molecule.[156] A similar complex can be formed with the two glutamines of the GXQ motifs near the transmembrane sequences TM2 and TM3. This assumption also takes into account that silicic acid is co-transported with sodium;[143] the sodium gradient acts as a driving force for the uptake of silicic acid. Binding of silicic acid to the conserved glutamine residues of the GXQ motifs in TM7 and TM8 and sodium (bound to an unknown binding site) would induce a conformational change of the transporter from an outward-facing conformation to the inward-facing conformation. This conformational change results in the release of silicic acid via the conserved glutamine residues near TM2 and TM3 into the intracellular space (Fig. 11B). Intracellularly, silicic acid may be bound to an unknown factor preventing the polymerization of oversaturated solutions of the molecule.[151] This model requires an (energy-dependent) mechanism to pump the sodium out of the cell (like in sponges). Alternatively, a coupling of the conformational change of the transporter with silica deposition might be possible.[156]

6.3 Silicic acid transport in chrysophycean algae

Recently a gene responsible for silicic acid transport in chrysophycean algae has been identified.[157] These algae originate from the Late Precambrian (about 600 Myr ago),[158] when siliceous sponges already occurred (about 600 Myr ago);[159] diatoms are evolutionarily younger (about 240 Myr ago).[160] The data revealed that the mechanism of silicon transport in chrysophycean algae is mediated by a SIT protein, like in diatoms.[157] It contains the conserved CML(I)D motif that is proposed to form the active center of the silicon transporter protein. This motif is present in the predicted polypeptide sequence of most but not all SITs studied (see above).[161] The C, M, and D residues of this motif has been proposed to bind a zinc ion that may be involved in binding and transport of silicic acid (see above).[153,154]

6.4 Silicic acid transporter of higher plants

The concentrations of silicic acid in groundwater solutions are typically below the solubility of quartz (6–12 ppm SiO_2). Therefore plants must concentrate silicic acid to exceed the solubility of amorphous silica (about 120 ppm SiO_2). The concentration of soluble silicic acid in soil in equilibrium with solid SiO_2 like quartz, cristobalite or amorphous silica can reach ~0.1-2.0 mM.[162] Silicon uptake by the roots occurs in the form of uncharged silicic acid.[163] The uptake of silicic acid by rice roots is an energy-dependent process which is inhibited by metabolic inhibitors (e.g., NaCN, dichlorophenoxy acetate and 2,4-dinitrophenol) and low temperature.[164-166] The silicic acid is then translocated - via the xylem - to the shoot, also in the form of monomeric silicic acid,[167,168] and finally to the leaf where it precipitates beneath the cuticle layer to form a silica-cuticle double layer, as well as a silica-cellulose double layer.[61,63] The concentration of monomeric silicic acid in the xylem sap of rice exceeds the concentration at which silicic acid normally polymerizes [$Si(OH)_4$ >2 mM].[168] The concentration of silicic acid increases further in the shoot through transpiration of water, resulting in the polymerisation of silicic acid and silica gel formation.[61]

The different ability of higher plant species to accumulate silicon has been explained by differences in the silicon uptake mechanisms of their roots.[61] The ability of plant species to accumulate silicon varies over a huge range. A comparative study of three plant species with low (tomato), medium (cucumber) and high (rice) levels of silicon accumulation revealed that the K_m value but not V_{max} of silicon uptake is similar in all three species and amounts to 0.15 mM; the V_{max} values increased from tomato to cucumber and rice.[166] These results suggest that all three plant species have a similar silicon transporter but the density of this transporter is different.

Recently, the gene encoding a silicon transporter has been isolated from rice.[169] This gene (*Lsi1*) which has been identified using a rice mutant defective in silicon uptake[165] comprises five exons and four introns.[170] The silicon transporter in higher plants (rice) is not a homolog of the silicon transporter in diatoms and sponges. The protein encoded by *Lsi1* belongs to the aquaporin family of

proteins.[169] Aquaporins are proteins forming water channels in cellular membranes. These proteins have also been identified and functionally characterized in freshwater sponges (*L. baicalensis*) but no evidence has been obtained that aquaporins are involved in uptake of silicic acid in sponge cells.[171] The deduced amino acid sequence of the rice silicon transporter comprises six transmembrane domains and, like aquaporins, two NPA motifs (Fig. 12).[169] The transporter is expressed in the plasma membrane of the exodermis and endodermis cells of the roots beside the Casparian strips which without a transporter, would not allow a free passage of silicic acid for further translocation to the shoot and leaf.

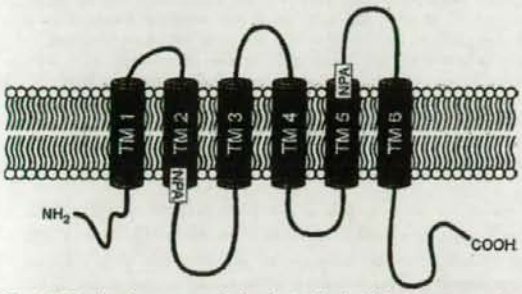

Fig. 12 Predicted structure of the plant (rice) silicic acid transporter comprising six transmembrane domains (TM1-TM6). The location of the two NPA motifs is shown. According to Ref. 63 with modifications.

The ability of Lsi1 to act as a silicon transporter was confirmed in microinjection experiments of Lsi1 RNA using frog (*X. laevis*) oocytes.[169] The transporter seems to be specific for silicic acid as revealed by competition experiments with glycerol.

The affinity for silicic acid of the transporter is relatively low (K_m = 0.15 - 0.3 mM). The uptake of silicic acid in plant (rice) cells is inhibited by phloretin, a nonspecific inhibitor of aquaporin-mediated transport of water and glycerol[172] but not DIDS,[173] an inhibitor of the sponge silicon transporter and other NBC transporters.

6.5 Silicic acid/silica uptake in vertebrates

A silicic acid transporter has not been identified in vertebrate cells although silicon has been shown to be an essential element in animals and human (see Section 3.4). However vertebrate cells are able to take up crystalline silica particles. Silica uptake in vertebrate cells appears to be mediated by surface-bound scavenger receptors. The primary receptor interacting with silica has recently been identified in alveolar macrophages from C57BL/6 mice. This receptor (macrophage receptor with collagenous structure, MARCO) is thought to be involved in silica cytotoxicity.[174]

7 Formation of organosilicon complexes: Polyols

Siliceous organisms like diatoms may contain high concentrations of soluble silicic acid, besides the deposited silica. The estimated concentration of soluble silicon of diatom cells is in the range of 19 - 340 mM (given as orthosilicic acid).[151] The solubility limit for orthosilicic acid is about 2 mM. Also sponges (silicasomes; see Section 8.1) might contain high concentrations of soluble silicic acid. Quantitative ^{29}Si MAS NMR experiments on diatoms revealed the existence of intracellular pools of less condensed silica; the Q^4:Q^3 ratios for complete cells are significantly smaller (1.8-1.9) than those for cell walls (2.5-2.8).[175] The mechanism by which diatoms can maintain such high concentrations of silicon in solution is not yet known. Chemically, this could be realized by generation of hypervalent silicon-containing molecules through complex formation. Stable six-coordinated silicon complexes can be formed between $H_3SiO_4^-$ and catechol (1,2-dihydroxybenzene), tropolone (2-hydroxy-2,4,6-cycloheptatrien-1-one) or 2-hydroxypyridine *N*-oxide. Formation of complexes ("chelates") of silica with catechol is favored at high pH, whereas the reaction with tropolone is favored at low pH. Formation of a complex, bis[citrato(3-)-O^1,O^2,O^6]silicate, with hexacoordinate silicon and two tridentate dioato(2-)olato(1-) ligands has been reported.[176] The formation of silica from tris(catecholato)silicate complexes, $(M^+)_2[Si(C_6H_4O_2)_3]$ (Scheme 3A) has been extensively studied by the group of C.C. Perry.[99,177]

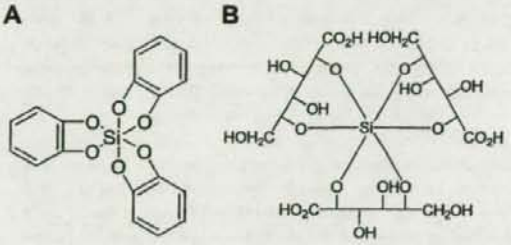

Scheme 3 Structure of the hexa-coordinated tris(catecholato)silicate (A) and tri[η^2-2,5-(+)-gluconato]silicate complex (B).

Silicic acid has been shown by the group of Kinrade also to form (water-stable) complexes with certain sugars or polyols.[102] Such molecules could indeed be identified inside cells of the diatom *Navicula pelliculosa* by ^{29}Si NMR spectroscopy.[104] Polyalcohols with at least four adjacent OH groups and *threo* configuration of the two middle OH groups (such as threitol, mannitol, sorbitol, and xylitol) are able to form stable five- and six-coordinated organosilicon complexes with silicate in aqueous alkaline solutions.[102] Such complexes are also formed by certain aliphatic acid carbohydrates (such as gluconic acid, saccharic acid and glucoheptonic acid);[178] the structure of the hexa-coordinated tri[η^2-2,5-(+)-gluconato]silicate complex is shown in Scheme 3B. The formation of hexa-coordinated species over both penta- and tetra-coordinated species is favoured at increasing pH or decreasing temperature. The affinity of complex-forming alcohols increases with increasing number of hydroxy groups.[103] The existence of stable alkoxy substituted silicate anions formed with these ligands in aqueous alkaline silicate solutions has been proved by ^{29}Si-NMR.[103] NMR studies even provided evidence for the existence of pentaoxo organosilicon complexes in dilute neutral aqueous silicate solutions.[179] Complexation of $H_3SiO_4^-$ ions with polyols enhances the

solubility of silica; under these conditions, stable silica solutions containing up to 3 mol l^{-1} silica can be prepared without gelation.[102] Formation of soluble 2/1 complexes of certain sugars with basic silicic acid in aqueous solution has also been reported by other groups.[180] The sugar silicates mainly consist of pentacoordinate silicate.

Carbohydrates may also play a potential role in silicate transport.[104,178]

8 Special aspects of sponge spicule formation

8.1 Demosponges

Primmorphs from the sponge *S. domuncula* were used to study spicule formation. Electron microscopical studies revealed that the initial steps of spicule formation and the formation of the first silica layer around a (short) the axial filament occur in vesicles of sclerocytes.[9] Small (up to 10 μm long) spicules are then extruded from the cells[9] and in the extracellular space, the spicules grow through apposition of lamellar silica layers up to a length of 450 μm and a diameter of 5 μm.[9,85] In the initial stage, the axial canal is primarily filled with the axial filament and additional string- and net-like structures which very likely represent clumped galectin.[12] In the final stage, it is almost completely filled with the axial filament, which displays the characteristic triangular form (Fig. 2B). Immunofluorescence studies revealed that silicatein exists both in the axial canal and on the surface of the spicules.[9,10,107]

Immunogold electron microscopical analysis showed that silicatein is present also in the extracellular space and arranged along galectin-containing strings, which are organized in parallel to the surfaces of the spicules.[9,12] In the presence of Ca^{2+}, silicatein binds to the galectin-containing strings allowing the appositional growth of the spicules. The silicatein/galectin-2 complexes are closely associated with the inorganic silica phase, both at the inner and the outer surface. The galectin-containing strings are organized by collagen fibers to net-like structures. These collagen fibers form an ordered network[12,181] and thereby control the spatial arrangement of the silicatein/galectin-2 complexes, i.e. the formation of concentric rings around the axis of a growing spicule (Fig. 13B) and the spicule shape.[9,10] The new silica lamellae are produced in hollow cylinders which have a diameter of 0.2 to 0.4 μm and are bordered by an outer net-like galectin layer with associated silicatein molecules and the surface of the spicule.[44] These tube-like cylinders are stabilized by collagen fibers.[181] The 1 to 3-μm thick lamellae are formed by silica nanoparticles with a diameter of about 100 to 200 nm, which are particularly visible in SEM images of partially etched spicules.[44] The assembly and packaging of the initially formed silica granules to form larger silica layers and the process (and the factors) which determines the species-specific shape of the spicules are not yet completely understood.

Further studies revealed that the spicules in the mesohyl are surrounded by sclerocytes[12,44,181] that, however, never come into close contact with the silica surface (Fig. 13A).[12,181] They are filled with electron-dense vesicles. Energy dispersive X-ray analysis showed that these vesicles have a high silicon content; they were termed silicasomes.[44] The silicasomes are released by the sclerocytes into the extracellular space and transported into the space around the spicules.

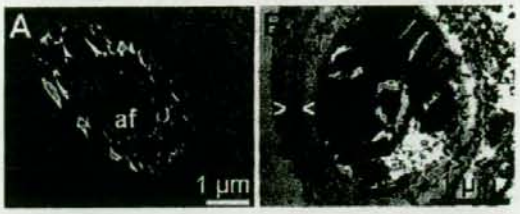

Fig. 13 (A) Cross-section through a spicule within a primmorph (*S. domuncula*) showing the axial canal (ac) with the triangular axial filament (af). The spicules are closely, but never intimately, associated by cells (sclerocytes). (B) Immunogold electron microscopy of a cross section through a growing spicule in primmorphs using polyclonal anti-silicatein antibodies. The immune complexes formed were visualized with nanogold anti-rabbit IgG. Concentric rings (><) are seen that surround the first layer of silica at the growing spicule. The silicatein-antibodies react with the axial filament and the silica-forming silicatein-galectin rings.

Based on these studies it has been thought that the silica lamellae are produced from silica released by silicasomes into the hollow cylinders around the growing spicules.[44] These silicasomes are produced in sclerocytes which accumulate silica within these vesicles through their $Na^+/HCO_3^-[Si(OH)_4]$ cotransporter. This model was also corroborated in biomimetical studies in which recombinant silicatein was immobilized on the surface of spicules freed of organic material, after functionalization with aminopropyltriethoxysilane (APS) and binding of a reactive ester polymer [poly(acetoxime methacrylate) to the primary amine created on the surface by APS treatment; this matrix was then used for immobilisation of His-tagged silicatein through Ni(II) complexation (Fig. 14A). Fourier transform infrared spectroscopy (FTIR) and electron microscopical (Fig. 14B) analysis revealed that new biosilica layers/lamellae deposited on the surface of the spicules are produced by the matrix-bound enzyme after incubation with substrate.[44]

8.2 Lithistids

Some siliceous sponge species, the lithistids, show an articulated skeleton. These sponges have hypersilicified spicules, so-called desmes, forming arms which interlock with each other.[182] The silica of the desmes of lithistid sponges consists of silica nanospheres which may fuse to form larger spheres.[182] It should be noted that hypersilicification of spicules can also occur in the presence of high concentrations of silicon. Maldonado *et al.*[183] presented experimental evidence that the concentration of silicon in seawater modulates the phenotypic expression of the various spicule types in a sponge species.

A special group of demosponges are keratose sponges which do not form their own spicules. These sponges may use foreign silica (sand) particles as inorganic skeletal material to stiffen their spongin fiber network.[184] In the keratose sponge, *Dysidea etheria*, active transport of silica particles to areas where skeletal fibers are formed have been observed.[185]

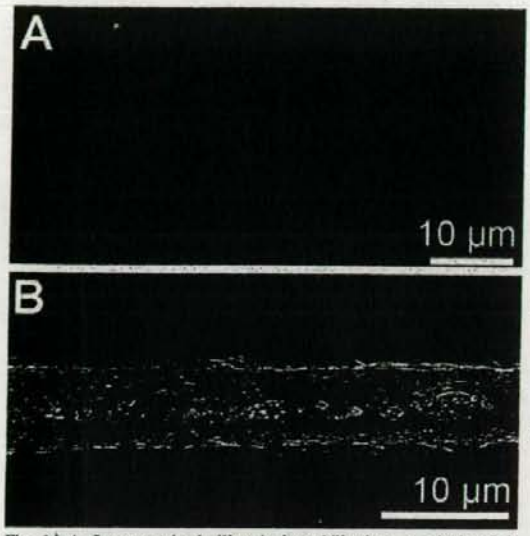

Fig. 14 A. Immunostained silicatein immobilized on a spicule of *S. domuncula*. B. SEM image of the biosilica layer formed by silicatein immobilized on *S. domuncula* spicule.

8.3 Hexactinellida

Hexactinellid sponges are characterized by a syncytial organization – in contrast to demosponges that have a cellular organization - and are the oldest sponge taxon as revealed by molecular biological[186] and geological data.[187] They evolved between two global glaciation ("snowball Earth")[188] periods 720-585 Myr ago (Neoproterozoic). The hexactinellid sponges form the largest biosilica structures known on Earth. For example, the giant spicules (basalia) of the deep sea hexactinellid *Monorhaphis chuni* have a length of up to 3 m and a maximum diameter of 8.5 mm.[189] In the center of these spicules a – compared to their diameter – relatively small axial canal (diameter, ~1 µm) is located which harbors the axial filament (see Fig. 2F). The cross-section of the axial filament in hexactinellid sponges is quadrangular, whereas the axial filaments in demosponges are triangular or hexagonal. The axial canal is surrounded by an electron dense, 100 to 150 µm-thick axial cylinder composed of silica. This - homogeneous - silica core structure is surrounded by up to 500 highly regularly arranged concentric silica lamellae.[189,190]

The siliceous skeleton of the hexactinellid sponge *Euplectella aspergillum* shows a hierarchical ordered structure.[191,192] At least six hierarchical levels in the length scale from nanometers to centimeters can be identified in the skeleton of *E. aspergillum*.[192,193] The mechanical properties of the spicules of *E. aspergillum* are influenced by the thin organic interlayers (5-10 nm) between the thicker concentric silica layers of the spicules.[194]

Recent studies indicate that the radial growth process of the hexactinellid spicules most likely occurs like in demosponges, although collagen is the predominant protein species of these spicules, which has an important influence on the physical-chemical / mechanical properties of this composite material.[190,195] Some physical-chemical properties of these spicules may also be influenced by their sodium and potassium contents which show regional variations as revealed by electron microprobe analysis.[190]

8.4 Optical fibers

Spicules from siliceous sponges, in particular spicules from the hexactinellid sponges *Rosella racovitzae*,[196] *E. aspergillum*[39] and *H. sieboldi*[197] turned out to be excellent light transmitters exhibiting some advantages over technical optical fibers.

The stalk spicules of *H. sieboldi* are composed of approximately 40 siliceous layers around the central axial filament and can reach 30 cm in length and a diameter of 300 µm (Fig. 2E). These spicules have been demonstrated to act as sharp high- and low pass filters. Only light with wavelengths between 615 nm and 1310 nm can pass through the spicule fiber, while wavelengths <615 nm and >1310 nm are filtered out.[197]

Investigations of the optical properties of the up to 15 cm long (diameter: up to 70 µm) basalia spicules of the hexactinellid sponge *E. aspergillum*[39,198] revealed a high refractive index in the core region, a low refractive index in the surrounding cylindrical tube, and a progressively increasing refractive index in the outer portion of the spicules. The differences in the refractive index could be explained by different contents of organic material and/or different degrees of hydration of the silica in the spicule core, the cylindrical tube and silica layers. In addition, the high refractive index in the core region may be caused by the enhanced concentration of sodium in this region.

The presence of lens-like structures at the end of the pentactinal spicules from the Antarctic hexactinellid sponge *R. racovitzae* has been shown to improve the light-collecting efficiency of the spicule optical fibers to collect ambient light;[196] this may allow delivery of sunlight to endosymbiotic algae.

Sponge spicules exhibit advantages over technical optical fibers: the composite structure of the sponge biosilica and the lamellar architecture of the spicule fibers, resulting in enhanced fracture toughness, the low-temperature synthesis, and the presence dopants (sodium) raising the refractive index of the fibers.

9 Model systems of biosilicification

A number of model systems have been used to study formation of biogenic silica nanostructures.[199] In principle, two different strategies can be applied;[200] *(i)* investigation of the effect on silica formation of biomolecules extracted from silica forming organisms, and *(ii)* study of the effect of model molecules which exhibit similar structural/functional properties to the natural occurring molecules (biomimetic approach). The first strategy has been used in most studies described above. Model molecules that have been used to mimic silica formation following the second strategy include amine-containing compounds (polyamines) such as spermine, spermidine, and putrescine homologues,[201,202] polyallylamine hydrochloride, polylysine and polyarginine,[23,203,204]

bifunctional molecules (e.g. cysteamine),[205] block copolypeptides (e.g. cysteine-lysine block copolypeptides),[206] and model biomolecules such as the R5 peptide (see Section 4.2.1).[122,123,207] Block copolypeptides contain covalently linked domains of water-soluble and water-insoluble polypeptides. These amphiphilic molecules are able to self-assemble into structured aggregates that display both hydrolytic and structure-directing activity, resulting in the formation of ordered silica structures from alkoxide substrates (TEOS). In addition, phage display libraries have been used as a further strategy to identify peptides showing silica forming activity.[208]

10 Biosilica and nanobiotechnology

The enzymes involved in silica metabolism, in particular silicatein[209] and silicase,[210] have attracted increasing attention because of their potential applications in the field of nanobiotechnology and biomedicine. Silica-based materials are used in many high-tech products including microelectronics, optoelectronics, and catalysts. Biocatalysis of silica formation from water soluble precursors, in particular silicatein-mediated biosilica production occurs under mild physiological conditions and is advantageous compared to technical (chemical) production methods applying high temperatures, pressures or extremes of pH. In addition, biological organisms like sponges and diatoms are able to fabricate their skeletons with high fidelity and in large copy number. These properties are of extreme importance for many applications in nano(bio)technology.

Silicatein remains functionally active even after immobilization of the protein onto metal or metal oxide surfaces.[109,211] Recombinant silicatein immobilized to a gold surface was able to catalyze the formation of interconnected silica nanospheres with a diameter about 70-300 nm.[81] The gold surface had been functionalized with the chelator nitrilotriacetic acid (NTA) alkanethiol which bound the recombinant His-tagged protein through Ni^{2+} complexation.[81] Binding of silicatein to metal or metal oxide surfaces was also achieved applying the method of self-assembled monolayers (SAM) formation.[212]

The range of potential applications of silicatein is increased by the fact that this enzyme is also able to catalyze - besides silica deposition - the (non-physiological) formation of other metal oxides like titania (TiO_2),[212-214], zirconia (ZrO_2),[212,215] and GaOOH/spinel gallium oxide[216] from the water stable precursors at room temperature and neutral pH. These metal oxides are known to exhibit semiconductor, piezoelectric, dielectric and/or electrooptic properties.

Based on these findings, new strategies towards the application of the silica forming enzymes have been designed. Biocatalytically (silicatein) formed silica may be used as coating of metal implants used in surgery (increase in biocompatibility), for the encapsulation of bioactive compounds (control of drug delivery) and in lithography (fabrication of microelectronics). For example, cultivation of bone-forming cells on silicatein (biosilica)-modified culture plates has been shown to result in an enhanced mineralization (formation of calcium phosphate) of the cells.[217] Thus biocatalytically formed silica may be applied in the production of bone-repairing materials and in dentistry. Silicatein has also been shown to catalyze the (ring-opening) polymerization of (cyclic) L-lactide to the biocompatible and biodegradable polymer poly(L-lactide) which is used as a scaffold in tissue engineering.[218]

Also the biosilica products formed by siliceous bioorganisms, e.g. the porous structures of diatom frustules may be used, e.g., for the construction of nanostructured membranes for particle separations.[219] Alternatively, functional analogues of the silica forming enzymes (silicatein) could be used to synthesize, e.g., micro- and mesoporous molecular sieves at room temperature and neutral pH.[220]

Silicatein also exhibits a reductive activity, which might be of technological interest; it catalyzes the reductive formation of colloidal gold nanoparticles which further aggregate to form gold nanocrystals, from tetrachloroaurate anions ($AuCl_4^-$) in solution.[211] His-tagged silicatein immobilized onto TiO_2 nanowires has been used to produce gold nanoparticles at the surface of the nanowires;[211] a multifunctional polymeric ligand containing dopamine/catechol (attachment of the polymer to the metal oxide surface) and NTA residues (binding of the His-tagged silicatein) has been applied. Following a similar approach, the fabrication of sponge spicule-like core-shell materials of alternating metal and metal oxide layers with complex properties was found to be feasible (Fig. 15).[109]

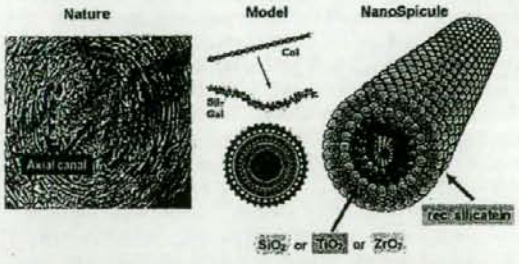

Fig. 15 (A) Tree ring structure of sponge spicules. (B) Nature as model: appositional growth of spicule around the axial (silicatein [green]) filament by formation of alternating organic (silicatein/galectin [Sil-Gal]) layers (organized by extra-spicular collagen [Col] fibrils) and inorganic (silica [yellow]) layers catalyzed by silicatein [green]. (C) Scheme highlighting the structure formation of amphiphile micelles (silicatein [green] + hydrophobic chain [grey]) which could be used for fabrication of artificial sponge spicules (silica [yellow]).

11 Conclusion

Biosilicifying organisms are capable of producing a huge variety of siliceous skeletal structures from nano scale to macro scale. In the past few years, first insights have been obtained into the mechanisms underlying biosilica formation and the molecules involved. New groups of enzymes (sponge silicateins) and proteins/polyamines (diatom silaffins) acting at the interface of inorganic chemistry and biochemistry have been discovered. The nanocomposite materials formed in particular by the sponge enzymes, silicatein and silicase

(protected by patents; silicatein,[209] and silicase[216]), are of extreme interest for application in nano(bio)technology;[221] thus nature is used as model to produce new nano-scale devices. The unique feature of biocatalytic (silicatein-mediated) silica formation is the possibility to produce silica glass under mild, low temperature and pressure, and near-neutral pH conditions; current methods require the application of high temperatures and pressures, and the use of caustic chemicals. This innovative technology will allow the production of metal oxide (silica and other metal oxides) coatings on organic (bio)material surfaces and the development of biomimetic fabrication procedures for new nanostructured materials and devices in opto- and microelectronics industry.[209,210,222,223] The enzymes involved in silica formation and degradation might also be of interest for organosilicon chemistry, in particular drug design (synthesis of new drug analogs by replacement of a specific carbon atom with a silicon atom; see Ref. 224).

12 Acknowledgements

This work was supported by grants from the European Commission, the Deutsche Forschungsgemeinschaft, the Bundesministerium für Bildung und Forschung Germany (project: Center of Excellence *BIOTEC*marin) and the International Human Frontier Science Program.

13 References

1 S. Mann, *Biomineralization: Principles and Concepts in Bioinorganic Materials Chemistry*, Oxford Chemistry Masters, Oxford University Press, 2001.
2 W. E. G. Müller (ed.) *Silicon Biomineralization: Biology, Biochemistry, Molecular Biology, Biotechnology*, Springer, Berlin, 2003, pp. 1-320.
3 C. C. Perry, *Rev. Mineral. Geochem.*, 2003, **54**, 291-327.
4 E. Bäuerlein, *Biomineralization*, Wiley-VCH, Cambridge, 2004.
5 P. Tréguer, D. M. Nelson, A. J. Van Bennekom, D. J. DeMaster, A. Leynaert and B. Quéguiner, *Science*, 1995, **268**, 375-379.
6 K. Shimizu, J. Cha, G. D. Stucky and D. E. Morse, *Proc. Natl. Acad. Sci. USA*, 1998, **95**, 6234-6238.
7 J. N. Cha, K. Shimizu, Y. Zhou, S. C. Christiansen, B. F. Chmelka, G. D. Stucky and D. E. Morse, *Proc. Natl. Acad. Sci. USA*, 1999, **96**, 361-365.
8 A. Krasko, B. Lorenz, R. Batel, H. C. Schröder, I. M. Müller and W. E. G. Müller, *Eur. J. Biochem.*, 2000, **267**, 4878-4887.
9 W. E. G. Müller, M. Rothenberger, A. Boreiko, W. Tremel, A. Reiber and H. C. Schröder, *Cell Tissue Res.*, 2005, **321**, 285-297.
10 W. E. G. Müller, S. I. Belikov, W. Tremel, C. C. Perry, W. W. C. Gieskes, A. Boreiko and H. C. Schröder, *Micron*, 2006, **37**, 107-120.
11 H. C. Schröder, A. Boreiko, M. Korzhev, M. N. Tahir, W. Tremel, C. Eckert, H. Ushijima, I. M. Müller and W. E. G. Müller, *J. Biol. Chem.*, 2006, **281**, 12001-12009.
12 W. E. G. Müller, S. I. Belikov, W. Tremel, U. Schloßmacher, A. Natoli, D. Brandt, A. Boreiko, M. N. Tahir, I. M. Müller and H. C. Schröder, in *Handbook of Biomineralization*, ed. E. Bäuerlein, vol. 1: The Biology of Biominerals Structure Formation, in press.
13 N. Kröger, C. Bergsdorf and M. Sumper, *EMBO J.*, 1994, **13**, 4676-4683.
14 M. Sumper, E. Brunner and G. Lehmann, *FEBS Lett.*, 2005, **579**, 3765-3769.
15 N. Kröger, R. Deutzmann and M. Sumper, *Science*, 1999, **286**, 1129-1132.
16 N. Kröger, R. Deutzmann, C. Bergsdorf and M. Sumper, *Proc. Natl. Acad. Sci. USA*, 2000, **97**, 14133-14138.
17 N. Kröger, S. Lorenz, E. Brunner and M. Sumper, *Science*, 2002, **298**, 584-586.
18 R. K. Iler, *The Chemistry of Silica*, John Wiley & Sons, New York, 1979.
19 C. C. Perry and T. Keeling-Tucker, *J. Biol. Inorg. Chem.*, 2000, **5**, 537-550.
20 B. Knoblich and T. Gerber, *J. Non-Cryst. Solids*, 2001, **283**, 109-113.
21 L. H. Allen and E. Matijevic, *J. Colloid Interface Sci.*, 1970, **33**, 420-429.
22 R. K. Iler, *J. Colloid Interface Sci.*, 1971, **37**, 364-373.
23 T. Mizutani, H. Nagase, N. Fujiwara and H. Ogoshi, *Bull. Chem. Soc. Jpn.*, 1998, **71**, 2017-2022.
24 T. Coradin and J. Livage, *Colloids Surf. B*, 2001, **21**, 329-336.
25 F. Fröhlich, Terra Nova, 1989, **1**, 267-273.
26 W. E. G. Müller, *Naturwissenschaften*, 1995, **82**, 321-329.
27 W. E. G. Müller, *Prog. Molec. Subcell. Biol.*, 1998, **19**, 89-132.
28 W. E. G. Müller, *Comp. Biochem. Physiol.*, 2001, **129A**, 433-460.
29 T. L. Simpson, *The Cell Biology of Sponges*, Springer-Verlag, New York, NY, 1984.
30 G. Holzhüter, K. Lakshminarayanan and T. Gerber, *Anal. Bioanal. Chem.*, 2005, **382**, 1121-1126.
31 E. G. Vrieling, T. P. M. Beelen, R. A. van Santen and W. W. C. Gieskes, *J. Phycol.*, 2000, **36**, 146-159.
32 G. Holzhüter, K. Narayanan and T. Gerber, *Anal. Bioanal. Chem.*, 2003, **376**, 512-517.
33 W. Arndt, in *Tabulae Biologicae*, ed. C. Oppenheimer and L. Pincussen, W. Junk, Berlin, 1930, pp. 39-120.
34 D. W. Schwab and R. E. Shore, *Biol. Bull.*, 1971, **140**, 125-136.
35 F. Sanford, *Micr. Res. Techn.*, 2003, **62**, 336-355.
36 W. E. G. Müller, O. V. Kaluzhnaya, S. I. Belikov, M. Rothenberger, H. C. Schröder, A. Reiber, J. A. Kaandorp, B. Manz, D. Mietchen and F. Volke, *J. Struct. Biol.*, 2006, **153**, 31-41.
37 M. J. Uriz, X. Turon and M. A. Becerro, *Progr. Molec. Subcell. Biol.*, 2003, **33**, 163-193.
38 M. J. Uriz, X. Turon, M. A. Becerro and G. Agell, *Micr. Res. Techn.*, 2003, **62**, 279-299.
39 J. Aizenberg, V. Sundar, A. D. Yablon, J. C. Weaver and G. Chen, *Proc. Natl. Acad. Sci. USA*, 2004, **101**, 3358-3363.
40 M. J. Uriz, *Can. J. Zool.*, 2006, **84**, 322-356.
41 M. J. Uriz, X. Turon and M. A. Becerro, *Cell Tissue Res.*, 2000, **301**, 299-309.
42 J. C. Weaver, L. I. Pietrasanta, N. Hedin, B. F. Chmelka, P. K. Hansma and D. E. Morse, *J. Struct. Biol.*, 2003, **144**, 271-281.
43 J. Weaver and D. E. Morse, *Micr. Res. Techn.*, 2003, **62**, 356-367.
44 H. C. Schröder, F. Natalio, I. Shukoor, W. Tremel, U. Schloßmacher, X. Wang and W. E. G. Müller, *J. Struct. Biol.*, in press.
45 N. Weissenfels and H. W. Landschoff, *Zool. Jahrb. Abt. Anat.*, 1977, **98**, 355-371.
46 N. Weissenfels, *Biologie und Mikroskopische Anatomie der Süßwasserschwämme (Spongillidae)*, Gustav Fischer Verlag, Stuttgart, 1989.
47 M. R. Custodio, I. Prokic, R. Steffen, C. Koziol, R. Borojevic, F. Brümmer, M. Nickel and W. E. G. Müller, *Mech. Ageing Develop.*, 1998, **105**, 45-59.
48 W. E. G. Müller, M. Wiens, R. Batel, R. Steffen, R. Borojevic and R. M. Custodio, *Marine Ecol. Progr. Ser.*, 1999, **178**, 205-219.
49 W. E. G. Müller, S. I. Belikov, O. V. Kaluzhnaya, S. Perović-Ottstadt, E. Fattorusso, A. Krasko and H. C. Schröder, *FEBS J.*, 2007, **274**, 23-36.
50 W. E. G. Müller, M. Wiens, T. Adell, V. Gamulin, H. C. Schröder and I. M. Müller, *Int. Rev. Cytol.*, 2004, **235**, 53-92.
51 H. C. Schröder, A. Krasko, G. Le Pennec, T. Adell, M. Wiens, H. Hassanein, I. M. Müller and W. E. G. Müller, *Prog. Mol. Subcell. Biol.*, 2003, **33**, 250-268.
52 H. C. Schröder, A. Krasko, R. Batel, A. Skorokhod, S. Pahler, M. Kruse, I. M. Müller and W. E. G. Müller, *FASEB J.*, 2000, **14**, 2022-2031.
53 H. C. Schröder, S. Perović-Ottstadt, M. Wiens, R. Batel, I. M. Müller and W. E. G. Müller, *Cell Tissue Res.*, 2004, **316**, 271-280.
54 R. Wetherbee, *Science*, 2002, **298**, 547.

55 E. G. Vrieling, W. W. C. Gieskes and T. P. M. Beelen, *J. Phycol.*, 1999, **35**, 548-559.
56 E. G. Vrieling, Q. Sun, T. P. Beelen, S. Hazelaar, W. W. Gieskes, R. A. van Santen and N. A. Sommerdijk, *J. Nanosci. Nanotechnol.*, 2005, **5**, 68-78.
57 C. E. Hamm, R. Merkel, O. Springer, P. Jurkojc, C. Maier, K. Prechtel and V. Smetacek, *Nature*, 2003, **421**, 841-843.
58 A. J. Milligan and F. M. Morel, *Science*, 2002, **297**, 1848-1850.
59 M. J. Hodson, P. J. White, A. Mead and M. R. Broadley, *Ann. Bot.*, 2005, **96**, 1027-1046.
60 E. Epstein, *Annu. Rev. Plant Physiol. Plant Mol. Biol.*, 1999, **50**, 641-664.
61 J. F. Ma and E. Takahashi, *Soil, Fertilizer, and Plant Silicon Research in Japan*, Elsevier, Amsterdam, 2002.
62 K. E. Richmond and M. Sussman, *Curr. Opin. Plant Biol.*, 2003, **6**, 268-272.
63 J. F. Ma and N. Yamaji, *Trends Plant Sci.*, 2006, **11**, 392-397.
64 S. Yoshida, *Bull. Natl. Inst. Agric. Sci. B*, 1965, **15**, 1-58.
65 J. A. Raven, *New Phytologist*, 2003, **158**, 419-430.
66 E. Epstein, *Proc. Natl. Acad. Sci. USA*, 1994, **91**, 11-17.
67 J. F. Ma, *Soil Sci. Plant Nutr.*, 2004, **50**, 11-18.
68 F. Fauteux, W. Remus-Borel, J. G. Menzies and R. R. Belanger, *FEMS Microbiol. Lett.*, 2005, **249**, 1-6.
69 F. P. Massey, A. R. Ennos and S. E. Hartley, *J. Anim. Ecol.*, 2006, **75**, 595-603.
70 M. Chérif, A. Asselin and R. R. Belanger, *Phytopathol.*, 1994, **84**, 236-242.
71 H. Kauss, K. Seehaus, R. Franke, S. Gilbert, R. A. Dietrich and N. Kröger, *Plant J.*, 2003, **33**, 87-95.
72 S. Sripanyakorn, R. Jugdaohsingh, R. P. H. Thompson and J. J. Powell, *Nutr. Bull.*, 2005, **30**, 222–230.
73 K. Schwarz and D. B. Milne, *Nature*, 1972, **239**, 333-334.
74 E. M. Carlisle, in *Biochemistry of Silicon and Related Problems*, ed. G. Bendz and I. Lingvist, 1978, pp. 231-253.
75 D. M. Reffitt, N. Ogston, R. Jugdaohsingh, H. F. Cheung, B. A. Evans, R. P. Thompson, J. J. Powell and G. N. Hampson, *Bone*, 2003, **32**, 127-135.
76 R. Jugdaohsingh, K. L. Tucker, N. Qiao, L. A. Cupples, D. P. Kiel and J. J. Powell, *J. Bone Miner. Res.*, 2004, **19**, 297-307.
77 K. I. Kivirikko and R. Myllyla, *Ann. N. Y. Acad. Sci.*, 1985, **460**, 187-201.
78 K. Schwarz, *Proc. Natl. Acad. Sci. USA*, 1973, **70**, 1608-1612.
79 E. M. Carlisle, *Ciba Found. Symp.*, 1986, **121**, 123-139.
80 D. M. Reffitt, R. Jugdaohsingh, R. P. Thompson and J. J. Powell, *J. Inorg. Biochem.*, 1999, **76**, 141-147.
81 M. N. Tahir, P. Théato, W. E. G. Müller, H. C. Schröder, A. Janshoff, J. Zhang, J. Huth and W. Tremel, *Chem. Commun.*, 2004, 848-2849.
82 N. Kröger, R. Deutzmann and M. Sumper, *J. Biol. Chem.*, 2001, 276, 26066-26070.
83 A. Krasko, H. C. Schröder, R. Batel, V. A. Grebenjuk, R. Steffen, I. M. Müller and W. E. G. Müller, *DNA Cell Biol.*, 2002, **21**, 67-80.
84 H. C. Schröder, S. Perović-Ottstadt, M. Rothenberger, M. Wiens, H. Schwertner, R. Batel, M. Korzhev, I. M. Müller and W. E. G. Müller, *Biochem. J.*, 2004, **381**, 665-673.
85 W. E. G. Müller, A. Krasko, G. Le Pennec, R. Steffen, M. Wiens, M. S. A. Ammar, I. M. Müller and H. C. Schröder, *Prog. Mol. Subcell. Biol.*, 2003, **33**, 195-221.
86 M. Pozzolini, L. Sturla, C. Cerrano, G. Bavestrello, L. Camardella, A. M. Parodi, F. Raheli, U. Benatti, W. E. G. Müller and M. Giovine, *Mar. Biotechnol.*, 2004, **6**, 594-603.
87 N. Funayama, M. Nakatsukasa, S. Kuraku, K. Takechi, M. Dohi, N. Iwabe, T. Miyata and K. Agata, *Zoolog. Sci.*, 2005, **22**, 1113-1122.
88 O. V. Kaluzhnaya, S. I. Belikov, H. C. Schröder, M. Wiens, M. Giovine, A. Krasko, I. M. Müller and W. E. G. Müller, *Naturwissenschaften*, 2005, **92**, 134-138.
89 M. Wiens, S. I. Belikov, O. V. Kaluzhnaya, A. Krasko, H. C. Schröder, S. Perovic-Ottstadt and W. E. G. Müller, *Dev. Genes Evol.*, 2006, **216**, 229-242.
90 A. Krasko, V. Gamulin, J. Seack, R. Steffen, H. C. Schröder and W. E. G. Müller, *Molec. Mar. Biol. Biotechnol.*, 1997, **6**, 296-307.
91 S. Gal and M. M. Gottesman, *Biochem. J.*, 1988, **253**, 303-306.
92 W. E. G. Müller, A. Krasko, G. Le Pennec and H. C. Schröder, *Microsc. Res. Tech.*, 2003, **62**, 368-377.
93 H. C. Schröder, S. Perović-Ottstadt, V. A. Grebenjuk, S. Engel, I. M. Müller and W. E. G. Müller, *Genomics*, 2005, **85**, 666-678.
94 W. E. G. Müller, S. I. Belikov and H. C. Schröder, *Science-First Hand*, 2006, **6**, 26-35.
95 W. E. G. Müller, H. C. Schröder, P. Wrede, O. V. Kaluzhnaya and S. I. Belikov, *J. Zool. Syst. Evol. Res.*, 2006, **44**, 105-117.
96 W. Stöber, A. Fink and E. Bohn, *J. Colloid Interface Sci.*, 1968, **26**, 62-69.
97 Y. Zhou, K. Shimizu, J. N. Cha, G. D. Stucky and D. E. Morse, *Angew. Chemie Int. Ed.*, 1999, **38**, 780-782.
98 D. F. Evans, J. Par and E. N. Coker, *Polyhedron*, 1990, **9**, 813-823.
99 C. C. Perry and Y. Lu, *J. Chem. Soc. Faraday Trans.*, 1992, **88**, 2915-2921.
100 C. C. Harrison and N. Loton, *J. Chem. Soc. Faraday Trans.*, 1995, **91**, 4287-4297.
101 C. C. Harrison, *Phytochemistry*, 1996, **41**, 37-42.
102 S. D. Kinrade, J. W. Del Nin, A. S. Schach, T. A. Sloan, K. L. Wilson and C. T. G. Knight, *Science*, 1999, **285**, 1542-1545.
103 S. D. Kinrade, K. J. Maa, A. S. Schach, T. A. Sloan and C. T. G. Knight, *J. Chem. Soc. Dalton Trans.*, 1999, **1999**, 3149-3151.
104 S. D. Kinrade, A. M. E. Gillson and C. T. G. Knight, *J. Chem. Soc. Dalton Trans.*, 2002, **2002**, 307-309.
105 G. Croce, A. Frache, M. Milanesio, L. Marchese, M. Causà, D. Viterbo, A. Barbaglia, V. Bolis, G. Bavestrello, C. Cerrano, U. Benatti, M. Pozzolini, M. Giovine and H. Amenitsch, *Biophys. J.*, 2004, **86**, 526-534.
106 S. V. Patwardhan, K. Shiba, H. C. Schröder, W. E. G. Müller, S. J. Clarson and C. C. Perry, *ASC Proceedings*, in press.
107 S. I. Belikov, O. V. Kaluzhnaya, H. C. Schröder, A. Krasko, I. M. Müller and W. E. G. Müller, *Cell Biol. Int.*, 2005, **29**, 943-951.
108 J. S. Mort, in *Handbook of Proteolytic Enzymes*, ed. A. J. Barrett, N. D. Rawlings and J. F. Woessner, Academic Press, Amsterdam, 2002, pp. 617-624.
109 H. C. Schröder, D. Brandt, U. Schlossmacher, X. Wang, M. N. Tahir, W. Tremel, S. I. Belikov and W. E. G. Müller, *Naturwissenschaften*, in press.
110 K. Tao, N. A. Stearns, J. Dong, Q. Wu and G. G. Sahagian, *Arch. Biochem. Biophys.*, 1994, **311**, 19-27.
111 G. Croce, D. Viterbo, M. Milanesio and H. Amenitsch, *Biophys. J.*, 2007, **92**, 288-292.
112 M. M. Murr and D. E. Morse, *Proc. Natl. Acad. Sci. USA*, 2005, **102**, 11657-11662.
113 A. J. Mort and D. T. A. Lamport, *Anal. Biochem.*, 1977, **82**, 289-309.
114 W. E. G. Müller, A. Borejko, D. Brandt, R. Osinga, H. Ushijima, B. Hamer, A. Krasko, C. Xupeng, I. M. Müller and H. C. Schröder, *FEBS J.*, 2005, **272**, 3838-3852.
115 G. Pohnert, *Angew. Chem. Int. Ed.*, 2002, **41**, 3167-3169.
116 M. Hildebrandt and R. Wetherbee, *Prog. Mol. Subcell. Biol.*, 2003, **33**, 11-57.
117 N. Kröger, C. Bergsdorf and M. Sumper, *Eur. J. Biochem.*, 1996, **239**, 259-264.
118 N. Kröger and M. Sumper, in *Biomineralization from Biology to Biotechnology and Medical Application*, ed. E. Bäuerlein, Wiley-VCH, Weinheim, 2000, pp 151-170.
119 N. Kröger, G. Lehmann, R. Rachel and M. Sumper, *Eur. J. Biochem.*, 1997, **250**, 99-105.
120 M. Wenzler, E. Brunner, N. Kröger, G. Lehmann, M. Sumper and H. R. Kalbitze, *J. Biomol. NMR*, 2001, **20**, 191-192.
121 S. Hazelaar, H. J. van der Strate, W. W. Gieskes and E. G. Vrieling, *Biomol. Eng.*, 2003, **20**, 163-169.
122 L. L. Brott, R. R. Naik, D. J. Pikas, S. M. Kirkpatrick, D. W. Tomlin, P. W. Whitlock, S. J. Clarson and M. O. Stone, *Nature*, 2001, **413**, 291-293.
123 R. R. Naik, P. W. Whitlock, F. Rodriguez, L. L. Brott, D. D. Glawe, S. J. Clarson and M. O. Stone, *Chem. Commun.*, 2003, **2**, 238-239.
124 V. V. Annenkov, S. V. Patwardhan, D. Belton, E. N. Danilovtseva and C. C. Perry, *Chem. Commun.*, 2006,1521-1523.

125 C. Wong Po Foo, S. V. Patwardhan, D. J. Belton, B. Kitchel, D. Anastasiades, J. Huang, R. R. Naik, C. C. Perry and D. L. Kaplan, *Proc. Natl. Acad. Sci. USA*, 2006, **103**, 9428-9433.

126 M. Sumper and G. Lehmann, *Chembiochem.*, 2006, **7**, 1419-1427.

127 K. M. Delak and N. Sahai, *Chem. Mater.*, 2005, **17**, 3221-3227.

128 M. Sumper, S. Lorenz and E. Brunner, *Angew. Chem. Int. Ed.*, 2003, **42**, 5192-5195.

129 E. Brunner, K. Lutz, M. Sumper, *Phys. Chem. Chem. Phys.*, 2004, **6**, 854-857.

130 K. Lutz, C. Groger, M. Sumper and E. Brunner, *Phys. Chem. Chem. Phys.*, 2005, **7**, 2812-2815.

131 M. Sumper, *Angew. Chem. Int. Ed.*, 2004, **43**, 2251-2254.

132 E. G. Vrieling, T. P. M. Beelen, R. A. van Santen and W. W. C. Gieskes, *Angew. Chem.*, 2002, **41**, 1543-1545.

133 C. C. Harrison and Y Lu, *Bull. Inst. Océanogr.*, 1994, **NS14**, 151-158.

134 C. C. Perry and T. Keeling-Tucker, *J. Colloid Polymer Science*, 2003, **281**, 652-664.

135 M. Maldonado, M. C. Carmona, Z. Velásquez, M. A. Puig, A. Cruzado, A. López and C. M. Young, *Limnol. Oceanogr.*, 2005, **50**, 799-809.

136 E. Gaino and M. Rebora, *Ital. J. Zool.*, 2003, **70**, 17-22.

137 W. S. Sly and P. Y. Hu, *Annu. Rev. Biochem.*, 1995, **64**, 375-401.

138 S. Hazelaar, Ph.D. Thesis, University of Groningen, Haren, The Netherlands, Van Denderen b.v., Groningen, 2006.

139 C. Gautier, J. Livage, T. Coradin and P. J. Lopez, *Chem. Commun.*, **2006**, 4611-4613.

140 D. M. Nelson, P. Tréguer, M. A. Brezinski, A. Leynaert and B. Quéguiner, *Glob. Biochem. Cycles*, 1995, **9**, 359-372.

141 V. Martin-Jézéquel, M. Hildebrand and M. A. Brzezinski, *J. Phycol.*, **36**, 821-840.

142 C. W. Sullivan, *J. Phycol.*, 1976, **12**, 390-396.

143 P. Bhattacharyya and B. E. Volcani, *Proc. Natl. Acad. Sci. USA*, 1980, **77**, 6386-6390.

144 S. Perović-Ottstadt, M. Wiens, H. C. Schröder, R. Batel, M. Giovine, A. Krasko, I. M. Müller and W. E. G. Müller, *J. Exp. Biol.*, 2005, **208**, 637-646.

145 D. W. Elvin, *Exp. Cell. Res.*, 1972, **72**, 551-553.

146 F. Azam, B. B. Hemmingsen and B. E. Volcani, *Arch. Mikrobiol.*, 1973, **92**, 11-20.

147 T. L. Simpson, L. M. Refolo and M. Kaby, *J. Morphol.*, 1979, **159**, 343-354.

148 T. L. Simpson, M. Gil, R. Connes, J. P. Diaz and J. Paris, *J. Morphol.*, 1985, **183**, 117-128.

149 M. Hildebrand, B. E. Volcani, W. Gassmann and J. I. Schroeder, *Nature*, 1997, **385**, 688-689.

150 M. Hildebrand, K. Dahlin and B. E. Volcani, *Mol. Gen. Genet.*, 1998, **260**, 480-486.

151 M. Hildebrand, in *Biomineralization*, ed. E. Bäuerlein, Wiley-VCH, Weinheim, 2000, pp. 171-186.

152 K. Thamatrakoln and M. Hildebrand, *Eukaryot. Cell*, 2007, **6**, 271-279.

153 T. A. Shcherbakova, Iu. A. Masiukova, T. A. Safonova, D. P. Petrova, A. L. Vereshchagin, T. V. Minaeva, R. V. Adel'shin, T. I. Triboi, I. V. Stonik, N. A. Aizdaicher, M. V. Kozlov, E. V. Likhoshvai and M. A. Grachev, *Mol. Biol. (Mosk.)*, 2005, **39**, 303-316.

154 M. Grachev, T. Sherbakova, Yu. Masyukova and Ye. Likhoshway, *Diatom Res.*, 2005, **20**, 409-411.

155 J. G. Rueter and F. M. M. Morel, *Limnol. Oceanogr.*, 1981, **26**, 67-73.

156 K. Thamatrakoln, A. J. Alverson and M. Hildebrand, *J. Phycol.*, 2006, **42**, 822-834.

157 Y. V. Likhoshway, Y. A. Masyukova, T. A. Sherbakova, D. P. Petrova and M. A. Grachev, *Dokl. Biol. Sci.*, 2006, **408**, 256-260.

158 A. H. Knoll, *Science*, 1992, **256**, 622-627.

159 J. Reitner and D. Mehl, *Geol. Paläont. Mitt. Innsbruck*, 1995, **20**, 335-347.

160 L. K. Medlin and I. Kaczmarska, *Phycologia*, 2004, **43**, 245-270.

161 E. V. Armbrust, J. A. Berges, C. Bowler, B. R. Green, D. Martinez, N. H. Putnam, S. Zhou, A. E. Allen, K. E. Apt, M. Bechner, M. A. Brzezinski, B. K. Chaal, A. Chiovitti, A. K. Davis, M. S. Demarest, J. C. Detter, T. Glavina, D. Goodstein, M. Z. Hadi, U. Hellsten, M. Hildebrand, B. D. Jenkins, J. Jurka, V. V. Kapitonov, N. Kröger, W. W. Lau, T. W. Lane, F. W. Larimer, J. C. Lippmeier, S. Lucas, M. Medina, A. Montsant, M. Obornik, M. S. Parker, B. Palenik, G. J. Pazour, P. M. Richardson, T. A. Rynearson, M. A. Saito, D. C. Schwartz, K. Thamatrakoln, K. Valentin, A. Vardi, F. P. Wilkerson and D. S. Rokhsar, *Science*, 2004, **306**, 79-86.

162 I. Gunnarsson and S. Arnórsson, *Geochimica Cosmochimica Acta*, 2000, **64**, 2295-2307.

163 E. Takahashi and K. Hino, *J. Sci. Soil Manure Jpn.*, 1978, **49**, 357-360.

164 A. Okuda and E. Takahashi, *J. Sci. Soil Manure Jpn.*, 1962, **33**, 453-455.

165 J. F. Ma, K. Tamai, M. Ichii and G. F. Wu, *Plant Physiol.*, 2002, **130**, 2111-2117.

166 N. Mitani and J. F. Ma, *J. Exp. Bot.*, 2005, **56**,1255-1261.

167 W. H. Casey, S. D. Kinrade, C. T. G. Knight, D. W. Rains and E. Epstein, *Plant Cell Environ.*, 2003, **27**, 51-54.

168 N. Mitani, J. F. Ma and T. Iwashita, *Plant Cell Physiol.*, 2005, **46**, 279-283.

169 J. F. Ma, K. Tamai, N. Yamaji, N. Mitani, S. Konishi, M. Katsuhara, M. Ishiguro, Y. Murata and M. Yano, *Nature*, 2006, **440**, 688-691.

170 J. F. Ma, N. Mitani, S. Nagao, S. Konishi, K. Tamai, T. Iwashita and M. Yano, *Plant Physiol.*, 2004, **136**, 3284-3289.

171 W. E G. Müller, S. I. Belikov, A. Krasko and H. C. Schröder, *Freshwater Biol.*, submitted.

172 R. I. Macey, *Am. J. Physiol.*, 1984, **246**, C195-C203.

173 K. Tamai and J. F. Ma, *New Phytol.*, 2003, **158**, 431-436.

174 R. F. Hamilton, S. A. Thakur, J. K. Mayfair and A. Holian, *J. Biol. Chem.*, 2006, **281**, 34218-34226.

175 R. Bertermann, N. Kröger and R. Tacke, *Anal. Bioanal. Chem.*, 2003, **375**, 630-634.

176 R. Tacke, M. Penka, F. Popp and I. Richter, *Eur. J. Inorg. Chem.*, 2002, **5**, 1025-1028.

177 C. C. Perry and T. Keeling-Tucker, *Chem. Commun.*, 1998, **1998**, 2587-2588.

178 S. D. Kinrade, R. J. Hamilton, A. S. Schach and C. T. G. Knight, *J. Chem. Soc. Dalton Trans.*, 2001, **2001**, 961-963.

179 S. D. Kinrade, A. S. Schach, R. J. Hamilton and C. T. Knight, *Chem. Commun.*, 2001, **17**, 1564-1565.

180 J. B. Lambert, G. Lu, S. R. Singer and V. M. Kolb, *Am. Chem. Soc.*, 2004, **126**, 9611-9625.

181 C. Eckert, H. C. Schröder, D. Brandt, S. Perovic-Ottstadt and W. E. G. Müller, *J. Histochem. Cytochem.*, 2006, **54**, 1031-1040.

182 A. Pisera, *Micrasc. Res. Techn.*, 2003, **62**, 312-326.

183 M. Maldonado, M. C. Carmona, M. J. Uriz and A. Cruzado, *Nature*, 1999, **401**, 785-788.

184 C. K. Teragawa, *J. Morph.*, 1986, **190**, 335-347.

185 C. K. Teragawa, *Biol. Bull.*, 1986, **170**, 321-334.

186 M. Kruse, I. M. Müller and W. E. G. Müller, *Mol. Biol. Evol.*, 1997, **14**, 1326-1334.

187 J. Reitner and G. Wörheide, in *Systema Porifera: A Guide to the Classification of Sponges*, ed. J. N. A. Hooper and R. W. M. Van Soest, Kluwer Academic/Plenum Publishers, New York, 2002, pp. 52-70.

188 F. A. Corsetti, A. N. Olcott and C. Bakermans, *Palaeogeography Palaeoclimatology Palaeoecology*, 2006, **232**, 114-130.

189 F. E. Schulze, *Hexactinellida. Wissenschaftliche Ergebnisse der Deutschen Tiefsee-Expedition auf dem Dampfer "Valdivia" 1898-1899*, Gustav Fischer Verlag, Stuttgart, 1904, pp. 1-266.

190 W. E. G. Müller, C. Eckert, K. Kropf, X. Wang, U. Schloßmacher, C. Seckert, S. E. Wolf, W. Tremel and H. C. Schröder, *Cell Tissue Res.*, in press.

191 J. Aizenberg, J. C. Weaver, M. S. Thanawala, V. C. Sundar, D. E. Morse and P. Fratzl, *Science*, 2005, **309**, 275-278.

192 J. C. Weaver, J. Aizenberg, G. E. Fantner, D. Kisailus, A. Woesz, P. Allen, K. Fields, M. J. Porter, F. W. Zok, P. K. Hansma, P. Fratzl and D. E. Morse, *J. Struct. Biol.*, in press.

193 J. D. Currey, *Science*, 2005, **309**, 253-254.

194 S. L. Walter, B. D. Flinn and G. Mayer, *Acta Biomater.*, in press.

195 H. Ehrlich, T. Hanke, P. Simon, C. Goebel, S. Heinmann, R. Born and H. Worch, *BIOmaterialien*, 2005, **6**, 297-302.
196 R. Cattaneo-Vietti, G. Bavestrello, C. Cerrano, A. Sarà, U. Benatti, M. Giovine and E. Gaino, *Nature*, 1996, **383**, 397-398.
197 W. E. G. Müller, K. Wendt, C. Geppert, M. Wiens, A. Reiber and H. C. Schröder, *Biosens. Bioelectron.*, 2006, **21**, 1149-1155.
198 V. C. Sundar, A. D. Yablon, J. L. Grazul, M. Ilan and J. Aizenberg, *Nature*, 2003, **424**, 899-900.
199 S. V. Patwardhan, S. J. Clarson and C. C. Perry, *Chem. Comm.*, 2005, **9**, 1113-1121.
200 P. J. Lopez, C. Gautier, J. Livage and T. Coradin, *Current Nanoscience*, 2005, **1**, 73-83.
201 D. Belton, S. V. Patwardhan and C. C. Perry, *Chem. Comm.*, 2005, **27**, 3475-3477.
202 D. J. Belton, S. V. Patwardhan and C. C. Perry, *J. Mater. Chem.*, 2005, **15**, 4629-4638.
203 D. Belton, G. Paine, S. V. Patwardhan and C. C. Perry, *J. Mater. Chem.*, 2004, **14**, 2231-2241.
204 M. M. Tomczak, D. D. Glawe, L. F. Drummy, C. G. Lawrence, M. O. Stone, C. C. Perry, D. J. Pochan, T. J. Deming and R. R. Naik, *J. Am. Chem. Soc.*, 2005, **127**, 12577-12582.
205 K. M. Roth, Y. Zhou, W. Yang and D. E. Morse, *J. Am. Chem. Soc.*, 2005, **127**, 325-330.
206 J. N. Cha, G. D. Stucky, D. E. Morse and T. J. Deming, *Nature*, 2000, **403**, 289-292.
207 M. R. Knecht and D. W. Wright, *Chem. Commun.*, 2003, **24**, 3038-3039.
208 R. R. Naik, L. L. Brott, S. J. Clarson and M. O. Stone, *J. Nanosci. Nanotech.*, 2002, **2**, 95-100.
209 *Europ. Pat.*, 1320624, 2004.
210 *Germ. Pat.*, 10246186, 2005.
211 M. N. Tahir, M. Eberhardt, H. A. Therese, U. Kolb, P. Theato, W. E. G. Müller, H. C. Schröder and W. Tremel, *Angew. Chem. Int. Ed.*, 2006, **45**, 4803-4809.
212 M. N. Tahir, P. Théato, W. E. G. Müller, H. C. Schröder, A. Borejko, S. Faiß, A. Janshoff, J. Huth and W. Tremel, *Chem. Commun.*, 2005, 5533-5535.
213 J. L. Sumerel, W. Yang, D. Kisailus, J. C. Weaver, J. H. Choi and D. E. Morse, *Chem. Mater.*, 2003, **15**, 4804-4809.
214 P. Curnow, P. H. Bessette, D. Kisailus, M. M. Murr, P. S. Daugherty and D. E. Morse, *J. Am. Chem. Soc.*, 2005, **127**, 15749-15755.
215 V. Bansal, D. Rautaray, A. Ahmad and M. Sastry, *J. Mater. Chem.*, 2004, **14**, 3303-3305.
216 D. Kisailus, J. H. Choi, J. C. Weaver, W. Yang and D. E. Morse, *Adv. Mater.*, 2005, **17**, 314-318.
217 H. C. Schröder, O. Boreiko, A. Krasko, A. Reiber, H. Schwertner and W. E. G. Müller, *J. Biomed. Mater. Res. Part B: Appl. Biomater.*, 2005, **75B**, 387-392.
218 P. Curnow, D. Kisailus and D. E. Morse, *Angew. Chem. Int. Ed. Engl.*, 2006, **45**, 613-616.
219 D. Losic, G. Rosengarten, J. G. Mitchell and N. H. Voelcker, *J. Nanosci. Nanotechnol.*, 2006, **6**, 982-989.
220 A. Corma, M. J. Diaz-Cabanas, M. Moliner and G. Rodriguez, *Chem. Commun.*, 2006, **29**, 3137-3139.
221 K. T. Ingemansson and M. Knezevic (eds.), *European Commission: 100 Technology Offers stemming from EU Biotechnology RTD results*, Directorate-General for Research, Office for Official Publications of the European Communities, Luxembourg, 2005, pp. 156-157.
222 D. Pisignano, G. Maruccio, E. Mele, L. Persano, F. Di Benedetto and R. Cingolani, *Appl. Physics Lett.*, 2005, **87**, 123109.
223 D. Kisailus, Q. Truong, Y. Amemiya, J. C. Weaver and D. E. Morse, *Proc. Natl. Acad. Sci. USA*, 2006, **103**, 5652-5657.
224 W. Bains and R. Tacke, *Curr. Opin. Drug Discov. Devel.*, 2003, **6**, 526-543.
225 M. Hildebrand, *Prog. Org. Coat.*, 2003, **47**, 256-266.

Retrovirology

BioMed Central

Research

Open Access

CD4-independent use of the CCR5 receptor by sequential primary SIVsm isolates

Anna Laurén*[1], Elzbieta Vincic[1], Hiroo Hoshino[2], Rigmor Thorstensson[3] and Eva Maria Fenyö[1]

Address: [1]Department of Laboratory Medicine, Division of Medical Microbiology/Virology, Lund University, Lund, Sweden, [2]Department of Virology and Preventive Medicine, Gunma University Graduate School of Medicine, Gunma, Japan and [3]Swedish Institute for Infectious Disease Control, Stockholm, Sweden

Email: Anna Laurén* - Anna.Lauren@med.lu.se; Elzbieta Vincic - Elzbieta.Vincic@med.lu.se; Hiroo Hoshino - Hoshino@med.gunma-u.ac.jp; Rigmor Thorstensson - Rigmor.Thorstensson@smi.ki.se; Eva Maria Fenyö - Eva_Maria.Fenyo@med.lu.se

* Corresponding author

Published: 23 July 2007

Retrovirology 2007, 4:50 doi:10.1186/1742-4690-4-50

Received: 22 March 2007

Accepted: 23 July 2007

This article is available from: http://www.retrovirology.com/content/4/1/50

Abstract

Background: CD4-independence has been taken as a sign of a more open envelope structure that is more accessible to neutralizing antibodies and may confer altered cell tropism. In the present study, we analyzed SIVsm isolates for CD4-independent use of CCR5, mode of CCR5-use and macrophage tropism. The isolates have been collected sequentially from 13 experimentally infected cynomolgus macaques and have previously been shown to use CCR5 together with CD4. Furthermore, viruses obtained early after infection were neutralization sensitive, while neutralization resistance appeared already three months after infection in monkeys with progressive immunodeficiency.

Results: Depending whether isolated early or late in infection, two phenotypes of CD4-independent use of CCR5 could be observed. The inoculum virus (SIVsm isolate SMM-3) and reisolates obtained early in infection often showed a pronounced CD4-independence since virus production and/or syncytia induction could be detected directly in NP-2 cells expressing CCR5 but not CD4 (CD4-independent-HIGH). Conversely, late isolates were often more CD4-dependent in that productive infection in NP-2/CCR5 cells was in most cases weak and was revealed only after cocultivation of infected NP-2/CCR5 cells with peripheral blood mononuclear cells (CD4-independent-LOW). Considering neutralization sensitivity of these isolates, newly infected macaques often harbored virus populations with a CD4-independent-HIGH and neutralization sensitive phenotype that changed to a CD4-independent-LOW and neutralization resistant virus population in the course of infection. Phenotype changes occurred faster in progressor than long-term non-progressor macaques. The phenotypes were not reflected by macrophage tropism, since all isolates replicated efficiently in macrophages. Infection of cells expressing CCR5/CXCR4 chimeric receptors revealed that SIVsm used the CCR5 receptor in a different mode than HIV-1.

Conclusion: Our results show that SIVsm isolates use CCR5 independently of CD4. While the degree of CD4 independence and neutralization sensitivity vary over time, the ability to productively infect monocyte-derived macrophages remains at a steady high level throughout infection. The mode of CCR5 use differs between SIVsm and HIV-1, SIVsm appears to be more flexible than HIV-1 in its receptor requirement. We suggest that the mode of CCR5 coreceptor use and CD4-independence are interrelated properties.

Background

Human immunodeficiency virus (HIV) and the simian counterpart, simian immunodeficiency virus (SIV) normally enter and infect cells after engagement with CD4 and a coreceptor, usually a chemokine receptor (reviewed by [1]). Binding to CD4 induces a conformational change to form and expose the coreceptor binding site. Further binding to the coreceptor induces additional rearrangements such that fusion between the viral envelope and the cell membrane can take place. The two major coreceptors used by HIV type-1 (HIV-1) are CCR5 and CXCR4 [2-4]. Viruses using the CCR5 coreceptor (R5-phenotype) predominate early in asymptomatic HIV-1 infection, while CXCR4-using HIV-1 (X4 phenotype) can be isolated in approximately half of the patients that progress to AIDS [5,6]. CCR5 is also the major coreceptor for SIV [7-9]. Furthermore, both HIV and SIV have been shown to use a wide set of alternative coreceptors, including CCR1, CCR2b, CCR3, CXCR6, CCR8, CX3CR1/V28, gpr1, gpr15, APJ, ChemR23 and RDC1, but the *in vivo* role of these coreceptors is still unknown [1].

CD4-independent use of coreceptors by HIV and SIV has long been an intriguing question. It has been assumed that CD4-independence is a sign of a more open envelope structure, more accessible to neutralizing antibodies and conferring altered cell tropism. HIV type 2 (HIV-2) and some SIV strains have been shown to enter cells independently of CD4 [10-14]. This was followed by reports on laboratory adapted HIV-1 variants that were able of CD4-independent infections [15-18]. CD4-independent HIV-1 was found to have a stable exposure of the coreceptor binding site [17]. However, similar conformational changes in the envelope have not yet been shown for SIV or HIV-2 and it may be that the HIV-1 envelope is more dependent on conformational changes for efficient infection than HIV-2 and SIV. Primary HIV-1 isolates that can infect cells independently of CD4 are rare and have not been isolated until lately [19]. However, Gorry *et al.* described a neurovirulent macrophage-tropic HIV-1 isolate that had increased affinity for CCR5 and could infect cells at minimal levels of CD4 [20]. Likewise, CD4-independence of SIV envelopes has been correlated to macrophage tropism and sensitivity to neutralization by heterologous sera or monoclonal antibodies [21,22]. Similar association between CD4-independent cell entry and sensitivity to neutralization has been reported for HIV-1 and HIV-2 [23-26]. Nevertheless, a thorough study of the relationships between macrophage tropism, neutralization sensitivity and CD4-independence of a large number of primary virus isolates has not yet been performed.

Our previous studies on CD4-independent use of CCR5 and gpr15 by envelopes of sequential SIVsm isolates (of sooty mangabey origin) showed that early reisolates from macaques infected with a CD4-independent inoculum maintained envelopes with a broad range of CD4-independent use of CCR5 in a fusion assay [27]. Envelopes from late reisolates at the time when the macaques had developed neutralizing antibodies were CD4-dependent. Infection with a CD4-dependent virus resulted in evolution to CD4-independence in late reisolates, indicating that CD4-dependent use of coreceptors may change in the course of infection [27]. Similarly, in two other studies, rapid progression of simian AIDS was accompanied by selection for CD4-independent variants [28,29]. Rapid disease was characterized by absent or transient humoral and cellular immune responses, high levels of virus replication and widespread dissemination of SIV in macrophages and multinucleated cells [28]. These studies did not, however, investigate macaques with a slow disease progression. Neither was neutralization sensitivity or macrophage tropism of the virus variants studied. This prompted us to investigate these issues in our material consisting of 13 cynomolgus macaques with different disease patterns. Sequential SIVsm isolates that previously have been characterized for coreceptor use and neutralization sensitivity were available [30,31]. All isolates, but one, used CCR5 for cell entry, and CCR5 was also the major coreceptor in 70 out of 105 isolates tested. Macrophage tropism, evaluated as relative replication capacity (relative to replication of SIVmac251) in monocyte-derived macrophages, coreceptor use and sensitivity to neutralization by autologous and heterologous sera, varied with severity of SIVsm infection. Long-term non-progressor (LTNP) macaques appeared to control virus in that virus isolates, if obtained at all, showed limited ability to use coreceptors late in infection [31]. On the other hand, reisolates from the majority of macaques with progressive disease maintained use of a wide variety of coreceptors and an effective replication capacity in macrophages throughout the 1–5 years study period. Furthermore, neutralization resistant variants emerged earlier in progressor macaques than in LTNP macaques [30]. In the present study we further analyse these isolates, focusing on CD4-independence, the mode of CCR5-use and macrophage tropism. We show that CD4-independent use of CCR5 and macrophage tropism are general properties of primary SIVsm isolates obtained from animals infected with a CD4-independent virus. CD4-independence is more pronounced early in infection than late. Phenotypic changes, like an increase in dependence on CD4 and neutralization resistance seem to occur earlier in progressor (P) and slow-progressor (SP) macaques than in LTNP animals while replication capacity in macrophages did not change during pathogenesis.

Results

CD4-independent infections of NP-2 cells

NP-2 cells expressing both CD4 and CCR5 were readily infected by CCR5-using (R5) SIVsm reisolates derived from virus isolation cultures with peripheral blood mononuclear cells (PBMC) of either macaque origin (mPBMC, 11 isolates) or human origin (hPBMC, 44 isolates) (data not shown). All isolates but one were previously shown to use CCR5 when tested on GHOST(3)-CCR5 and U87.CD4-CCR5 cells [31]. One isolate derived by cocultivation on hPBMC used CXCR4 and CXCR6 only (12-month isolate from macaque D24) and could not infect NP-2 cells expressing CD4 and CCR5. Clinical status of the macaques and description of the virus isolates are supplemented [see Additional file 1].

CD4-independent use of CCR5 was tested in two ways. First, NP2/CCR5 cells were infected and culture supernatants tested for reverse transcriptase (RT) activity and cultures observed for syncytia formation. Isolates which were positive using one or both of these parameters were defined as the phenotype CD4-independent-HIGH. However, it is possible that the absence of CD4 might reduce the amount of syncytia and therefore it was important to analyse infection by additional techniques. To explore whether the virus production and syncytia negative NP-2/CCR5 cultures were infected at all, we followed a second strategy. Infected cultures were trypsinized 7 days after infection, cells were washed once with PBS and added to new culture plates together with PHA-P stimulated hPBMC. Another six days later, supernatants were collected and analyzed for reverse transcriptase activity. The phenotype of isolates that were positive for CD4-independent use of CCR5 only after coculture with PBMC was defined as CD4-independent-LOW. Surprisingly, the SIVmac 32H isolate, known to use CCR5 independently of CD4, was of CD4-independent-LOW phenotype (Figure 1). Our results showed that, indeed, a majority of viruses were able to use CCR5 independently of CD4 to enter cells. However, infection of cells expressing CCR5 together with CD4 was at all times more effective than infection of cells expressing only CCR5.

Comparison of isolates obtained on monkey and human PBMC showed that viruses isolated on mPBMC had more often CD4-independent-HIGH phenotype than viruses isolated on hPBMC. In fact, the majority (seven out of eleven) of viruses isolated on mPBMC was of CD4-independent-HIGH phenotype and induced both syncytia and virus production in the NP-2/CCR5 cells (Table 1). The remaining four isolates obtained on mPBMC appeared to be CD4-independent-LOW. Isolation on hPBMC distinguished these phenotypes in a time-dependent manner (Figure 1). Accordingly, early isolates (defined as 2-week and 3 or 4-month isolates) from 11 macaques out of 13

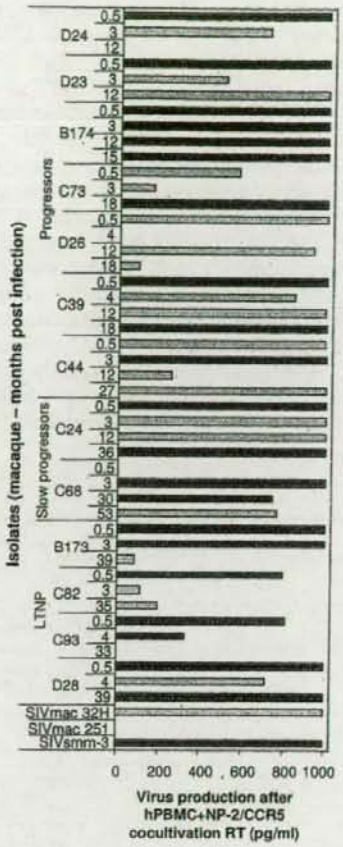

Figure 1
CD4-independent use of CCR5 by isolates obtained on hPBMC. NP-2/CCR5 cells were infected with virus stocks containing 2.7–3.5 log10 pg RT/well. The day after infection cultures were washed extensively and fresh medium was added. Infected NP-2/CCR5 cells were followed for syncytia induction up to seven days after infection. RT was analyzed in supernatants from NP-2 cells at day 1 after wash and before start of cocultivation. Cocultivation of NP-2/CCR5 cells with hPBMC was started seven days after infection and virus production was measured after additional 6 days. CD4-independent-HIGH, virus production and/or syncytia induction could be detected directly in NP-2/CCR5 cells (dark grey). CD4-independent-LOW, productive infection in NP-2/CCR5 cells revealed only after cocultivation of infected NP-2/CCR5 cells with hPBMC (light grey). RT was analyzed with undiluted supernatants and therefore values above 1.000 pg RT/ml cannot be separated. Detection limit for RT was 50 pg/ml. Values are means of duplicate infections.

and late isolates (defined as 12-month and/or later isolates) from only five macaques (out of 13) were able to induce syncytia and/or produce RT in NP-2/CCR5 cells (CD4-independent HIGH). However, when considering the difference between the two matched proportions (sequential early and late isolates) the difference was not statistically significant (p = 0.0703, two sided McNemar's test). McNemar's test measures the number of changes comparing matched early and late time-points and significant proportions were not reached due to the small number of samples. Phenotypes of sequential isolates changed in six animals from CD4-independent-HIGH to CD4-independent-LOW, while isolates from four animals appeared CD4-independent-HIGH both early and late in infection. Change in phenotype from CD4-independent-LOW to CD4-independent-HIGH was only observed in one animal and in two macaques the CD4-independent-LOW phenotype did not seem to change throughout infection.

Considering changes of CD4-independence in relation to disease progression, phenotypic changes seemed to occur slower in LTNP macaques than in P and SP macaques. As early as two-weeks after infection four out of nine macaques with progressive disease harbored viruses that had changed to CD4-independent-LOW. In contrast, virus isolated from the four LTNP macaques was of the CD4-independent-HIGH phenotype, the same phenotype as that of the inoculum virus. At three or four months after infection CD4-independent-HIGH viruses were still isolated in two out of four LTNP animals, while only three out of nine macaques from the P and SP group harbored viruses with the CD4-independent-HIGH phenotype. CD4-independence of the P and SP group was fluctuating and at the last time point four out nine macaques were CD4-independent-HIGH. In contrast, in LTNP macaques virus evolution was narrowed further and the CD4-independent-HIGH phenotype was only apparent in one out of four macaques.

Table 1: Comparison of the capacity to infect NP-2 cells by isolates on mPBMC or hPBMC.

Origin of cells for virus isolation	Isolate[a]			NP-2/CD4/CCR5 syncytia[b]	NP-2/CCR5 syncytia	NP-2/CCR5+PBMC virus production [c] RT (pg/ml)
	Monkey	Time PI (months)				
mPBMC	D24	0.5		++++	+++	>1000
		3		++++	+	803
		10	§	+++	-	560
	C73	5	§	++++	++	>1000
		7	§	++++	++	649
		18		++++	+	450
	C68	0.5	#	++	-	526
		30	#	++	-	674
		53	#	++	-	78
	B173	0.5		++++	+++	998
		39		++++	+	827
hPBMC	D24	0.5		+++	-	>1000
		3		++	-	713
		12	§	-	-	<50
	C73	0.5	§	++	-	573
		3	§	++	-	161
		18		++++	-	>1000
	C68	0.5		++++	-	<50
		3	§	++++	-	>1000
		30		++++	-	741
		53		++++	-	762
	B173	0.5		++++	+/-	>1000
		90	§	++	-	>1000
		39		+	-	85

[a] Cells were infected with virus stocks containing 2.7–3.5 log10 pg RT/well except for indicated (#) isolates that were infected with 1.9–2.3 log10 pg RT/well. §Isolates that could not be obtained on corresponding time-points when isolating viruses on mPBMC and hPBMC, respectively. PI, time for virus isolation post infection.

[b] Induction of syncytia was observed in light microscope 5 and 7 days after infection. -, no syncytia; +, 10–20 syncytia per well; ++, syncytia covering 20–50% of the wells; +++, syncytia covering 50–90% of the wells; ++++, syncytia covering >90% of the wells

[c] Virus production was measured six days after start of cocultures with human PBMC (hPBMC). Values are means of two independent infections in duplicate wells. Supernatant culture fluids were collected at day 7 and production of RT was analyzed. Supernatants were undiluted in the RT assay and therefore values above 1000 pg RT/ml cannot be separated. Cut-off detection level was 50 pg RT/ml

Intracellular and extracellular virus maturation

HIV-1 virions can assemble and mature intracellularly within macrophages and retain infectivity for several weeks [32]. This prompted us to test whether viruses had matured intracellularly in the NP-2/CCR5 cells and upon cocultivation transferred to hPBMC in a cell-to-cell fashion. To study possible intracellular virus assembly and maturation, the infected NP-2 cells were detached with trypsin and washed with PBS, lysed by the addition of 0.001% Triton X-100 and one cycle of freeze-thawing. Visual inspection in the light microscope and culturing attempts showed that cell lysis was complete. The lysates were then titrated on hPBMC. Presence of intracellular virus was demonstrated in infections of NP-2/CCR5 cells with 11 out of 19 isolates tested (Figure 2). It is possible that the lysis procedure affected the infectivity of viruses and this could account for the negative cultures. Interestingly, the majority of virus isolates that established infection in hPBMC after infection with lysed cells were of the CD4-independent-HIGH phenotype. Similar lysis experiments were not performed with NP-2/CD4/CCR5 cell lines because these infections showed stronger cytopathic effect (large syncytia and pronounced cell death) than NP-2/CCR5 cultures.

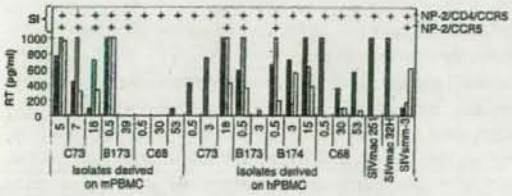

Figure 2

Intracellular and extracellular virus maturation shown by infection of hPBMC with lysates and supernatants of NP-2/CCR5 cultures. Seven days after infection, NP-2 cells were trypsinized, washed with PBS and lysed by 0.001% Triton X-100 followed by one cycle of freeze-thawing step. Lysates were titrated at five-fold dilution steps on hPBMC. Supernatant culture fluids from hPBMC infections were collected at day 7 and production of RT was analyzed with undiluted supernatants. The RT cut-off detection level was 50 pg/ml and values above 1000 pg/ml could not be separated. Dark grey bars represent mean virus production in NP-2/CD4/CCR5 cells and. light grey bars represent virus production in NP-2/CCR5 cells. White bars represent virus production measured by RT in PBMC infected with cell lysates diluted 1:5 from infected NP-2/CCR5 cells. Positive syncytia induction (SI) are indicated with +. Means of RT production in duplicates of infection are indicated.

Mode of CCR5 use

To further dissect CCR5-use by SIV, the mode of CCR5-use was evaluated in U87.CD4 cell lines expressing chimeric receptors constructed of CCR5 and CXCR4 (Figure 3) [33]. In the present experiments we used three chimeras (FC-1, FC-2 and FC-4b), in which CCR5 had been exchanged gradually, beginning with the N-terminal, for corresponding parts of the CXCR4 molecule. FC-1 and FC-2 differ in the first transmembrane portion, which is CCR5 in FC-1 and CXCR4 in the FC-2 chimera. The CXCR4 portion of FC-4b extends to the fourth transmembrane region. The U87.CD4 cell line is known to endogenously express other SIV coreceptors (GPR1 and CXCR6) known to be used by SIV [34,35] and to control for possible GPR1 or CXCR6 use, the U87.CD4 parental cell line was included in all experiments. No syncytia induction or viral antigen production was observed in the U87.CD4 parental cells in parallel infections with the SIVsm isolates (data not shown). Our results showed that the FC-1 receptor was frequently used by SIVsm (93% of the hPBMC reisolates) and FC-2 and FC-4b were also used by a high number of isolates (78% and 71% of hPBMC reisolates, respectively, Figure 3). However use of FC-2 and FC-4b was rarely as effective as FC-1 use. Interestingly, the 12-month isolates from macaque D24 which has an unusual X4X6 phenotype [31] was only able to use FC-4b among the panel of chimeric receptors used in this study. Twenty-nine out of 45 of the hPBMC reisolates and eight out of 11 of the mPBMC reisolates could use all three chimeric receptors. There was no relationship between the isolates capacity to infect cells with the different chimeric receptors and disease progression of the animals.

Replication in human and macaque MDM

Reisolates from all monkeys (45 isolates derived on hPBMC) could readily infect human MDM (Figure 4). The majority of isolates replicated efficiently and showed high virus production in supernatants 15 days after infection (values above 5000 pg/ml). Also the SIVsm isolate SMM-3 that was used to infect the macaques replicated efficiently (14111 pg RT/ml). A few isolates showed lower replication efficacy (range 460 to 4185 pg RT/ml) and these isolates also widely varied in replication in MDM from different blood donors. A comparison between five virus isolates obtained on monkey as well as human PBMC showed similar replication capacities in monkey MDM (data not shown). Performing the same experiment on MDM of human origin showed that isolates obtained on macaque PBMC tended to replicate to lower levels (range 595 to 2100 pg RT/ml) relative to isolates obtained on human PBMC (range 1770 to 23732 pg RT/ml). Nevertheless, the hierarchy of replication capacities among isolates was the same (data not shown). Due to the limited availability of macaque blood we could not perform all experiments with cells from macaque origin.

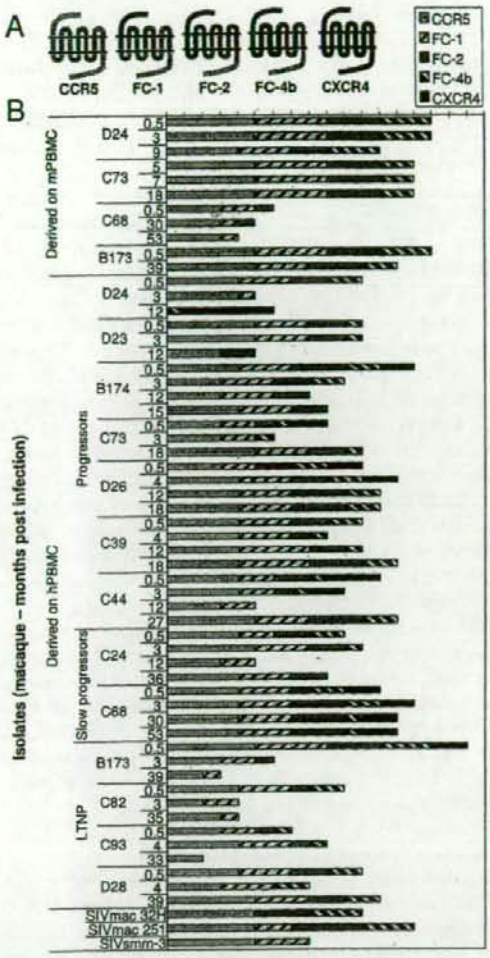

Figure 3
Mode of CCR5-use. A. Schematic figure of CCR5 and the chimeric receptors FC-1, FC-2 and FC-4b. The CCR5 part is represented as grey and the CXCR4 part as black. B. Mode of CCR5-use was analyzed by infection of U87.CD4 cells expressing CCR5 or chimeric receptors. Length of bars indicates degree of infection and syncytia induction as observed in a light microscope 5 and 7 days after infection. Degree of infection follows a scale from 0 to 5 where 0 is no syncytia and RT negative; 1 was <10 syncytia per well or RT positive; 2 was 10–20 syncytia per well; 3 indicates syncytia covering 20–50% of the wells; 4 indicates syncytia covering 50–90% of the wells; 5 indicates syncytia covering >90% of the wells. RT production was positive in grades ranging from 2 to 5 and in concordance with syncytia induction.

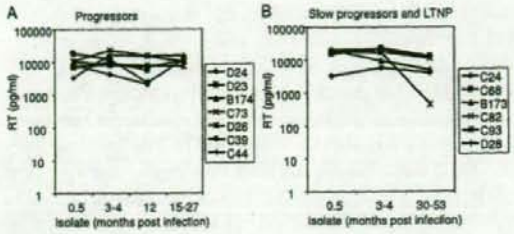

Figure 4
Replication capacity in macrophages of viruses isolated on hPBMC from progressors (A) versus slow progressors and LTNP (B). Macrophages were infected with virus stocks containing 3.0–3.1 log10 pg RT/well (in 88% of the cultures) and RT production was measured in MDM 15 days after infection. Values are means from at least two experiments with MDM from different donors.

We also evaluated replication capacity in macrophages relative to the first isolate of each macaque as an alternative to observe changes in macrophage-tropism over-time. We found that the relative differences for macrophage-tropism when comparing early and late isolates was in the range of 1 to 4.8-fold as measured by virus production in macrophages day 15 (with one exception (monkey C93) the difference was 28-fold). However, changes in macrophage tropism could not be correlated to progression of disease.

CD4-independent use of CCR5 and neutralization sensitivity of SIVsm isolates

We asked the question if CD4-independence of the SIVsm reisolates evaluated in this study correlated with neutralization sensitivity, evaluated previously [30]. For this purpose we compared CD4-independence and neutralization sensitivity evaluated as neutralization by a high titer serum (H55:16) from a LTNP macaque (Figure 5). Similar changes in neutralization sensitivity were also evident when tested by autologous sera [30]. Two parameters, CD4-independence and neutralization sensitivity allowed us to examine early and late isolates for phenotypic changes. The results show that early in infection CD4-independent-HIGH and neutralization sensitive populations were in majority, since reisolates from all four LTNP and five out of nine SP/P macaques showed this phenotype. A few months later this population decreased (two out of nine P/SP macaques and two out of four LTNP macaques) and virus populations with CD4-independent-LOW and neutralization sensitive phenotypes expanded. In one P animal a CD4-independent-HIGH and neutralization resistant phenotype appeared already three months after infection and this population became prevalent at late stages in the P/SP group.

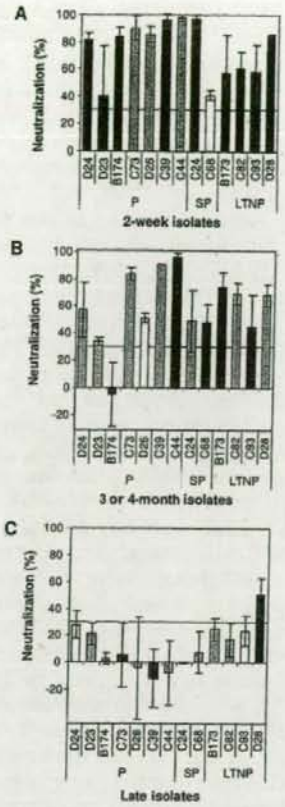

Figure 5

CD4-independence and neutralization sensitivity. Phenotypic changes in CD4-independence and sensitivity of neutralization over-time in 13 macaques. Neutralization sensitivity of three isolates (A, 2-week isolates, B, 3 or 4-month isolates and C, late isolates) from each macaque was tested with 1:20 dilution of serum [30]. Neutralization was also performed with autologous serum which gave similar results (data not shown). Neutralization sensitivity was measured using the GHOST(3) cell plaque reduction assay which has a cut-off for neutralization at 30% (marked with a line), that is results below 30% are negative [67]. The majority of newly infected macaques harbored virus populations with a CD4-independent-HIGH (dark grey bars) and neutralization sensitive phenotype. This phenotype gradually changed to become a CD4-independent-LOW (light grey bars) and neutralization resistant (below 30%) virus population. CD4-dependent isolates (white bars) were seen in both neutralization sensitive and neutralization resistant populations. Values are mean neutralization (+/- SD) of two independent assays performed in triplicates.

Discussion

Sequential SIVsm reisolates from 13 macaques with different disease progression were monitored for CD4-independent use of CCR5, mode of CCR5-use and replication capacity in macrophages. The majority of reisolates was capable of CD4-independent infection in NP-2/CCR5 cells and could replicate efficiently in macrophages. However, productive infection in NP-2 cells expressing CCR5 but not CD4 was in most cases revealed only after coculti-vation of infected NP-2/CCR5 cells with hPBMC (CD4-independent-LOW). In comparison, infection of NP-2 cells expressing both CD4 and CCR5 resulted in more efficient syncytia induction and productive infection. Also the SMM-3 inoculum was capable of CD4-independent use of CCR5 and replicated well in macrophages. Reisolates obtained early in infection (2-week isolates from nine macaques and 3 or 4-month isolates from four macaques) showed a more pronounced CD4-independence (CD4-independent-HIGH) since virus production and/or syncytia induction could be detected directly in NP-2/CCR5 cells. Late isolates, especially from LTNP macaques, were more restricted in CD4-independent infections. This is in line with our previous study in which we showed that envelope clones from early SIVsm reisolates maintained a broad range of CD4-independence when the macaques were infected with a CD4-independent inoculum virus [27]. In the same study, CD4-dependence increased in late reisolates from macaques that developed neutralizing antibodies to the inoculum virus and to the early isolates.

Based on studies of CD4-independent laboratory-adapted variants of HIV-1, Hoffman and co-workers suggested that envelopes capable of binding to coreceptors in a CD4-independent manner are likely to have a "more open" conformation, similar to CD4-triggered CD4-dependent envelopes [17]. For SIV Chen *et al.* showed that the crystal structure of unligated envelope from CD4-independent SIVmac 32H needed to refold and move parts of the envelope 40 Å in order to reveal the structure of the coreceptor binding site known from the CD4-ligated HIV-1 HXBc2 envelope previously crystallized by Kwong *et al.* [36,37]. Many studies have shown an association between CD4-independence and neutralization sensitivity for HIV as well as SIV [21-26]. However, in these studies correlation between CD4-independence and neutralization sensitivity was based on fusion assays of pseudoviruses with expression of various cloned envelopes. In the present study, we used primary isolates that consist of a swarm of viruses expressing different envelopes and closer reflect the *in vivo* situation than cloned envelopes. We have previously shown with the material included in the present study that the 2-week isolates were neutralization sensitive while the 3 or 4-month isolates and especially late isolates evolved to neutralization resistance [30]. Likewise,

CD4-independent use of CCR5 is more pronounced with virus isolates obtained shortly after infection of the macaques. Thus, newly infected macaques often harbored virus populations with a CD4-independent-HIGH and neutralization sensitive phenotype (Figure 5). At two weeks after infection the CD4-independent-HIGH phenotype was observed in isolates from approximately half of the P and SP macaques, while at the same time-point this was the only phenotype present in LTNP macaques. Gradual change to a CD4-independent-LOW and neutralization resistant virus population was evident and faster in progressors than LTNP macaques. This can be interpreted as a sign of a more open envelope conformation early as compared to late virus populations. Interestingly, in the P/SP group of macaques there was also a fraction of animals that late in infection had a CD4-independent-HIGH and neutralization resistant phenotype. Selection of CD4-independent variants has also previously been shown to occur in macaques with rapid progression of simian AIDS [28,29] and was characterized by absent or transient humoral and cellular immune responses [28]. Thus, it appears that CD4-independent use of CCR5 evolves in different directions in progressors and LTNP macaques. It is tempting to speculate that in LTNP macaques the overall immunity is more potently controlling the virus. Loss of immune control in progressors may lead to variants with a more CD4-independent and open conformation of the envelope.

CD4-independence of SIV envelopes have previously been correlated not only to neutralization sensitivity but to macrophage tropism as well [21,22]. Moreover, since macrophages have a lower CD4-expression than T lymphocytes it has been suggested that this would influence their susceptibility to HIV or SIV infection [38-41]. In the present study we found a clear correlation between CD4-independent use of CCR5 and macrophage tropism, inasmuch all isolates productively infected macrophages and also infected cells expressing CCR5 but not CD4 as shown by cocultivation of infected NP-2/CCR5 cells with hPBMC, infection of hPBMC with lysates and supernatants from infected NP-2/CCR5 cells. Thus, the majority of the SIVsm isolates were both macrophage-tropic and CD4-independent. However, the correlation between CD4-independence and macrophage-tropism was not strict since some of the isolates that appeared negative for CD4-independence even after cocultivation of NP-2/CCR5 and hPBMC could replicate to high levels in macrophages.

In infected MDM, virus particles can be observed within intra-cytoplasmic vesicles with characteristic multivesicular bodies known as late endosomes or major histocompability complex class II compartments [42,43]. Similarly and recently, reports have shown that large amounts of infectious virions accumulate in endosomal compartments within 293 T cells, in chronically infected human T lymphocytes [44]and as well as in primary macrophages [32]. Viruses accumulated intracellularly in macrophages can retain infectivity for at least 6 weeks shown by infection of MAGI cells with cell lysates from infected macrophages [32]. In the present study we found that in SIVsm-infected NP-2/CCR5 cells virus can mature intracellularly as shown by infection of hPBMC with cell lysates from infected cells. Virus production was also detected after contact of NP-2/CCR5 cells with hPBMC. It is tempting to speculate that the low or non-productive infection of non-CD4-expressing cells may be amplified by contact with T-lymphocytes *in vivo*. The importance of direct cell-to-cell spread in HIV infections is well known [45-47]. However, we also have to consider the possibility that the NP-2/CCR5 cell line is not infected and that viruses are only taken up by the NP-2/CCR5 cells in a fashion similar to that of DC-SIGN and transferred to PBMC after cocultivation [48,49]. Dentritic cells (DC) have been shown to capture and internalize extracellular HIV or SIV via DC-SIGN or DC-SIGNR and, without being infected, transmit virus to T cells *in trans*. In our system, we could show that infection of NP-2/CCR5 cells expressing CCR5 with CD4-independent-HIGH isolates resulted in a low level virus production seven days after infection and we could also observe syncytia induction in these cells. Interestingly, the compartment where HIV is captured by DC after DC-SIGN uptake has been shown to be similar to the multivesicular bodies where intracellular assembly and budding occurs in macrophages [50,51]. Transmission of HIV between cells has been shown to occur in an infectious or virological synapse that locally concentrates virus and receptors between infected and uninfected cells [52-55]. Ganesh *et al.* showed that viruses transferred by this synapse are poorly accessible to neutralizing antibodies [53]. Accordingly, when viruses assemble, bud and mature in endosomal compartments, this may provide means for cell to cell transfer of virus without encountering the immune system.

Mode of CCR5 receptor use may affect the virus-receptor interaction at entry. A high number of our SIVsm isolates could use all three chimeric CCR5-CXCR4 receptors included in this study. FC-1, with only the extracellular N-terminal exchanged for CXCR4 was the most commonly used chimera. This is in contrast with the results of Edinger *et al.* who showed that the N-terminal of CCR5 is the critical domain for CD4-independent entry of SIVsm envelope clones [56]. This group also found that the N-terminal of CCR5 in chimeric CCR2b/CCR5 chemokine receptors was sufficient for entry into CD4+ cells of the M-tropic strain SIVmac316 and, by contrast, the strains SIVmac239 and SIVmac251 required the presence of the second extracellular loop of CCR5 and exhibited a